Electronic Supplementary Information

Copper(I) 5-phenylpyrimidine-2-thiolate complexes showing unique optical properties and high visible light-directed catalytic performance

Meng-Juan Zhang,[a] Hong-Xi Li,*[a] Hai-Yan Li[a] and Jian-Ping Lang*[a,b]

[a] State and Local Joint Engineering Laboratory for Novel Functional Polymeric Materials, College of Chemistry, Chemical Engineering and Materials Science, Soochow University, Suzhou 215123, Jiangsu, People's Republic of China.

[b] State Key Laboratory of Organometallic Chemistry, Shanghai Institute of Organic Chemistry, Chinese Academy of Sciences, Shanghai 200032, People's Republic of China

Table of contents

Synthesis of [(5-phpyms)$_2$Cu]$_n$. To a Pyrex glass tube were added CuBr (3.6 mg, 0.025 mmol), 5-phpymtH (4.7 mg, 0.025 mmol), 2 mL of MeCN and 0.1 mL of DMSO. The tube was sealed and heated in an oven at 120 ºC for 48 h and then cooled to room temperature at the rate of 5 ºC h^{-1} to form a large amount of blue crystals of [(5-phpyms)$_2$Cu]$_n$, which were collected by filtration, washed with Et_2O and dried in air. Yield: 6.1 mg (46 %). Anal. Calcd (%) for $C_{20}H_{14}CuN_4O_6S_2$: C 44.98, H 2.64, N 10.49. Found: C 44.54, H 2.81, N 10.62. IR (KBr pellet, ν/cm^{-1}): 3059 (w), 1586 (w), 1454 (w), 1429 (m), 1285 (s) 1229 (w), 1211 (w), 1192 (w), 1007 (s), 778 (m), 764 (m), 642 (m).

X-ray Crystallography for [(5-phpyms)$_2$Cu]$_n$. Single crystal of [(5-phpyms)$_2$Cu]$_n$ suitable for X-ray analysis was obtained directly from the above preparations. The crystal data were collected on a Bruker APEX-II CCD using an enhanced X-ray source Mo Kα (λ = 0.71073 Å). Single crystal of [(5-phpyms)$_2$Cu]$_n$ was mounted on glass fibers with grease cooled in a liquid nitrogen stream at 273 K. The collected data were reduced by using the program *Bruker APEX2* and an absorption correction (multi-scan) was applied. The reflection data were also corrected for Lorentz and polarization effects. The crystal structure of [(5-phpyms)$_2$Cu]$_n$ was solved by direct methods and refined on F^2 by full-matrix least-squares methods with the *SHELXL-97* program.[S1] All non-H atoms were refined anisotropically. All other hydrogen atoms were placed in the geometrically idealized positions and constrained to ride on their parent atoms. Crystallographic data for the structural analysis have been deposited with the Cambridge Crystallographic Data Centre, CCDC No. 1474578.

Crystal Structure of [Cu(5-phpyms)$_2$]$_n$. Compound [Cu(5-phpyms)$_2$]$_n$ crystallizes in the monoclinic space group $P2_1/c$, and its asymmetric unit contains half a discrete [Cu(5-phpyms)$_2$] unit. Compound [Cu(5-phpyms)$_2$]$_n$ has a 1D chain (extending along the *b* axis) in which each Cu atom is bridged by two pairs of 5-phpyms ligands (Fig. S1). Each 5-phpyms in [Cu(5-phpyms)$_2$]$_n$ takes a μ_3-κ^1(N)-κ^1(O)-κ^1(O') chelating/bridging mode to bind at two Cu atoms. Each Cu adopts an octahedral geometry defined by four O and two N from four 5-phpyms ligands. Cu(1)-N(2) bond distance is close to that in [$CuBr_2$(dpds)] (dpds = 2,2'-dipyridyldisulfide).[S2] Cu(1)-O(1) bond length is much shorter than the Cu(1)-O(2A) bond distance and that in [Cu(en)$_2$(1,5-nds)·2H_2O]$_n$ (2.8128(13) Å; 1,5-nds = naphthalenedisulfonate)[S3] and {[Cu_3(L)$_2$(py)$_{12}$]·py}$_n$ (2.461(3) Å; H_3L = 1,3,5-Tri(4-sulfonophenyl)-benzene).[S4]

Table S1 Selected bond lengths (Å) and angles (º) of **1**·2MeCN, **2**-**5** and $[(5\text{-phpyms})_2Cu]_n$

Complex **1**·2MeCN

Cu(1)-N(4)	1.9943(15)	Cu(1)-S(3)	2.2619(5)
Cu(1)-S(1)	2.2635(5)	Cu(2)-N(2)	2.0287(15)
Cu(2)-S(2)	2.2304(5)	Cu(2A)-S(3)	2.2865(5)
Cu(3)-N(5)	2.0236(15)	Cu(3)-S(2)	2.2248(5)
Cu(3A)-S(1)	2.2820(5)	Cu(2A)···Cu(3)	3.0335(4)
Cu(1)···Cu(2)	2.7758(4)	Cu(1)···Cu(3)	2.8388(4)
N(4)-Cu(1)-S(3)	128.33(5)	N(4)-Cu(1)-S(1)	131.09(5)
S(3)-Cu(1)-S(1)	99.082(18)	N(2)-Cu(2)-S(2)	133.54(5)
N(2)-Cu(2)-S(3A)	109.93(5)	S(2)-Cu(2)-S(3A)	110.535(19)
N(5)-Cu(3)-S(2)	133.38(4)	N(5)-Cu(3)-S(1A)	110.57(4)
S(2)-Cu(3)-S(1A)	112.145(19)		

Complex **2**

Br(1)-Cu(1)	2.4256(8)	Cu(1)-N(1)	2.022(3)
Cu(1)-S(2)	2.2342(13)	Cu(2)-N(3)	1.987(3)
Cu(2)-S(1)	2.2327(13)	Cu(2)-S(2A)	2.3582(14)
Cu(1)-Cu(2)	2.6444(8)		
N(1)-Cu(1)-S(2)	138.82(11)	N(1)-Cu(1)-Br(1)	103.48(10)
S(2)-Cu(1)-Br(1)	117.69(4)	N(3)-Cu(2)-S(1)	137.38(11)
N(3)-Cu(2)-S(2A)	111.29(11)	S(1)-Cu(2)-S(2A)	109.47(5)

Complex **3**

Cu(1)-N(3A)	1.958(7)	Cu(1)-S(1A)	2.177(2)
Cu(1)-S(1)	2.670(2)	Cu(2)-N(1)	2.040(7)
Cu(2)-S(2)	2.268(2)	Cu(2)-Br(1)	2.6028(13)
Cu(2)-Br(2)	2.6365(14)	Cu(3)-N(4B)	2.020(7)
Cu(3)-S(1A)	2.245(2)	Cu(3)-S(2)	2.529(2)
Cu(3)-Br(1)	2.5591(14)	Cu(4)-N(2C)	1.991(7)
Cu(4)-S(2D)	2.229(2)	Cu(4)-Br(2)	2.4295(14)
Cu(4)···Cu(3E)	2.7794(17)	Cu(1)···Cu(1A)	2.527(2)
Cu(2)···Cu(1A)	2.7040(16)	Cu(2)···Cu(3)	3.0058(16)
N(3A)-Cu(1)-S(1A)	141.6(2)	N(3A)-Cu(1)-S(1)	97.9(2)
S(1A)-Cu(1)-S(1)	118.12(7)	N(1)-Cu(2)-S(2)	157.9(2)
N(1)-Cu(2)-Br(1)	91.6(2)	S(2)-Cu(2)-Br(1)	106.59(7)
N(1)-Cu(2)-Br(2)	101.6(2)	S(2)-Cu(2)-Br(2)	89.74(6)
Br(1)-Cu(2)-Br(2)	94.11(4)	N(4B)-Cu(3)-S(1A)	153.0(2)
N(4B)-Cu(3)-S(2)	94.8(2)	S(1)-Cu(3)-S(2A)	108.27(8)
N(4B)-Cu(3)-Br(1)	102.2(2)	S(1)-Cu(3)-Br(1A)	87.58(7)
S(2)-Cu(3)-Br(1)	100.42(7)	N(2C)-Cu(4)-S(2D)	135.7(2)

N(2C)-Cu(4)-Br(2)	105.66(19)	S(2)-Cu(4)-Br(2D)	118.36(7)

Complex **4**

I(1)-Cu(1)	2.6611(10)	I(1)-Cu(2)	2.8103(10)
Cu(1)-N(1)	1.984(5)	Cu(1)-S(2A)	2.2061(19)
Cu(2)-N(3)	2.039(5)	Cu(2)-S(1A)	2.252(2)
Cu(2)-Cu(1A)	2.5678(12)	Cu(2)-I(1A)	2.7715(11)
Cu(2)-Cu(2A)	2.997(2)	Cu(1)-Cu(1B)	2.9539(18)
N(1)-Cu(1)-S(2A)	130.20(16)	N(1)-Cu(1)-I(1)	112.66(15)
S(2A)-Cu(1)-I(1)	115.78(6)	N(3)-Cu(2)-S(1A)	134.03(17)
N(3)-Cu(2)-I(1A)	98.66(15)	S(1A)-Cu(2)-I(1A)	114.75(6)
N(3)-Cu(2)-I(1)	102.05(14)	S(1A)-Cu(2)-I(1)	91.77(5)
I(1A)-Cu(2)-I(1)	115.06(4)		

Complex **5**

I(1)-Cu(2)	2.5891(9)	I(1)-Cu(1)	2.9383(10)
Cu(1)-N(1)	1.968(6)	Cu(1)-S(1A)	2.2239(16)
Cu(2)-I(2)	2.5496(16)	Cu(1)-Cu(1A)	2.741(2)
Cu(2)-Cu(2B)	2.665(3)	Cu(1)-Cu(2)	2.6508(14)
N(1)-Cu(1)-S(1A)	149.26(16)	N(1)-Cu(1)-I(1)	103.57(16)
S(1A)-Cu(1)-I(1)	105.19(7)	I(2)-Cu(2)-I(1)	119.88(3)
I(2)-Cu(2)-I(1B)	119.88(3)	I(1)-Cu(2)-I(1B)	118.06(5)

Complex $[(5\text{-phpyms})_2Cu]_n$

Cu(1)-N(2)	1.975(7)	Cu(1) O(1)	1.988(6) . ?
Cu(1)-O(2A)	2.414(6)	Cu(1) O(2A)	87.1(3)
N(2)-Cu(1)-O(1B)	94.4(3)	N(2B) Cu(1) O(1B)	85.6(3)
N(2)-Cu(1)-O(1)	85.6(3)	N(2B) Cu(1) O(1)	94.4(3)
O(1B)-Cu(1)-O(1)	180.000(3)	N(2) Cu(1) O(2C)	92.9(3)
N(2B)-Cu(1)-O(2C)	87.1(3)	O(1B) Cu(1) O(2C)	90.3(2)
O(1)-Cu(1)-O(2C)	89.7(2)	N(2) Cu(1) N(2B)	180.000(1)
N(2B)-Cu(1)-O(2A)	92.9(3)	O(1B) Cu(1) O(2C)	89.7(2)
O(1)-Cu(1)-O(2A)	90.3(2)	O(2C) Cu(1) O(2A)	180.000(1)

Symmetry codes: (A) 1 - x, 1 – y, 1 - z for **1**·2MeCN. (A) - x, 1 – y, 2 - z for **2**. (A) - x, 1 – y, 1 - z ; (B) - x, – y, 1 – z; (C) 1 - x, 1 – y, 1 – z; (D) 1 - x, – y, 1 – z; (E) 1 + x, y, z for **3**. (A) -x, 5/2 + y, 3/2 - z, (B) 1 - x, 5/2 + y, 3/2 - z for **4**. (A) x, -y, 1 + z; (B) -x, +y, 1 - z for **5**. (A) x, 1 + y, z, (B) 1 - x, 5/2 + y, 3/2 - z, (C) 1 - x, 3/2 + y, 3/2 - z for $[(5\text{-phpyms})_2Cu]_n$.

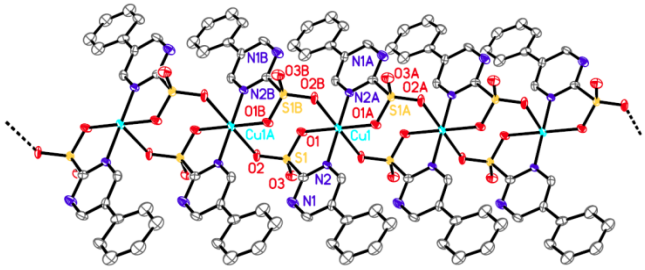

Fig. S1 View of a portion of the 1D chain of $[Cu(5\text{-phpyms})_2]_n$ extending along the *b* axis.

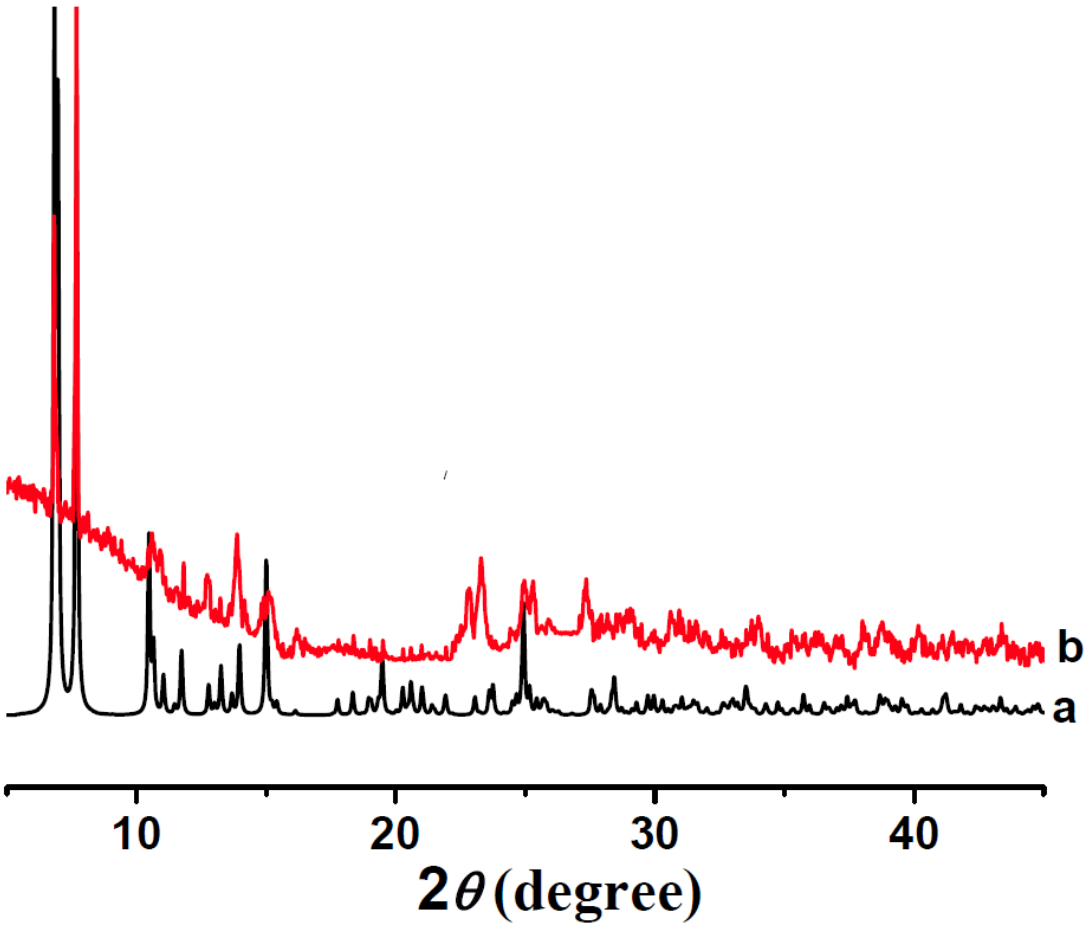

Fig. S2 PXRD patterns for **1**. (a) simulated; (b) a single-phase polycrystalline sample of **1**.

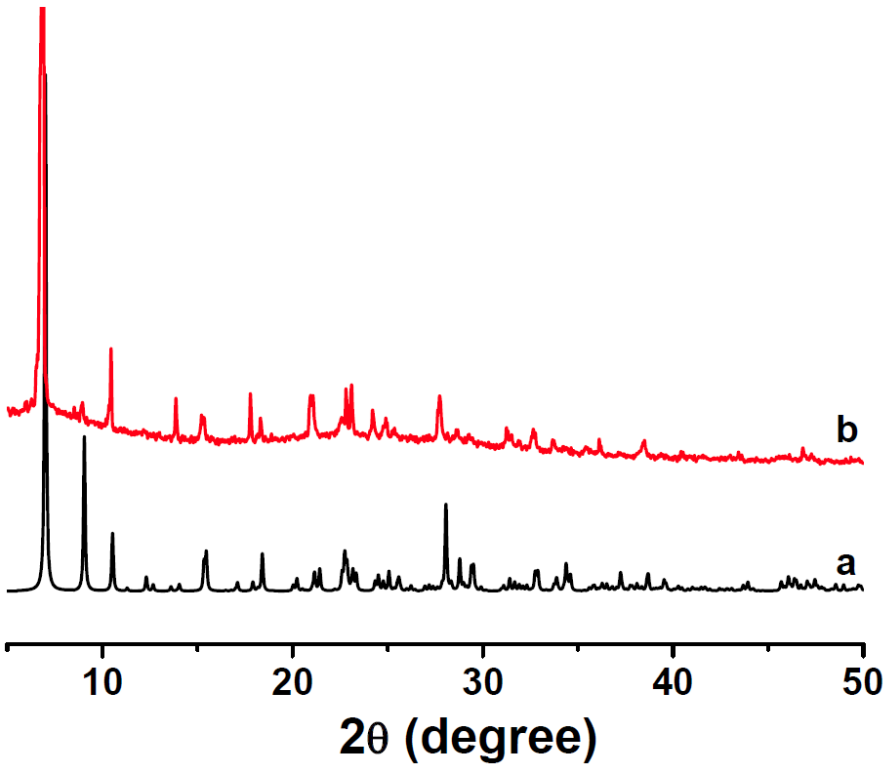

Fig. S3 PXRD patterns for **2**. (a) simulated; (b) a single-phase polycrystalline sample of **2**.

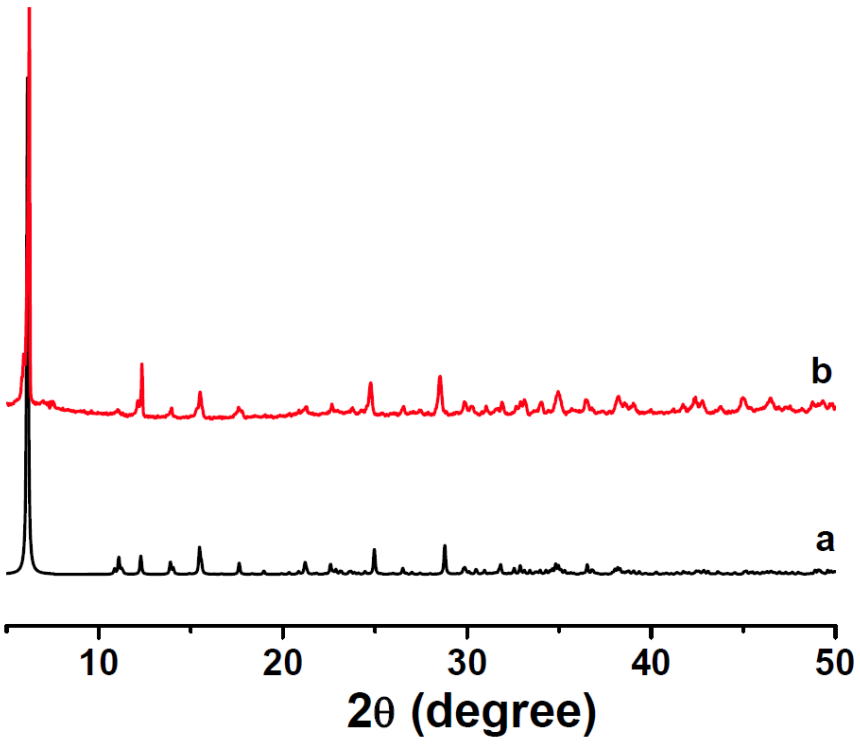

Fig. S4 PXRD patterns for **3**. (a) simulated; (b) a single-phase polycrystalline sample of **3**.

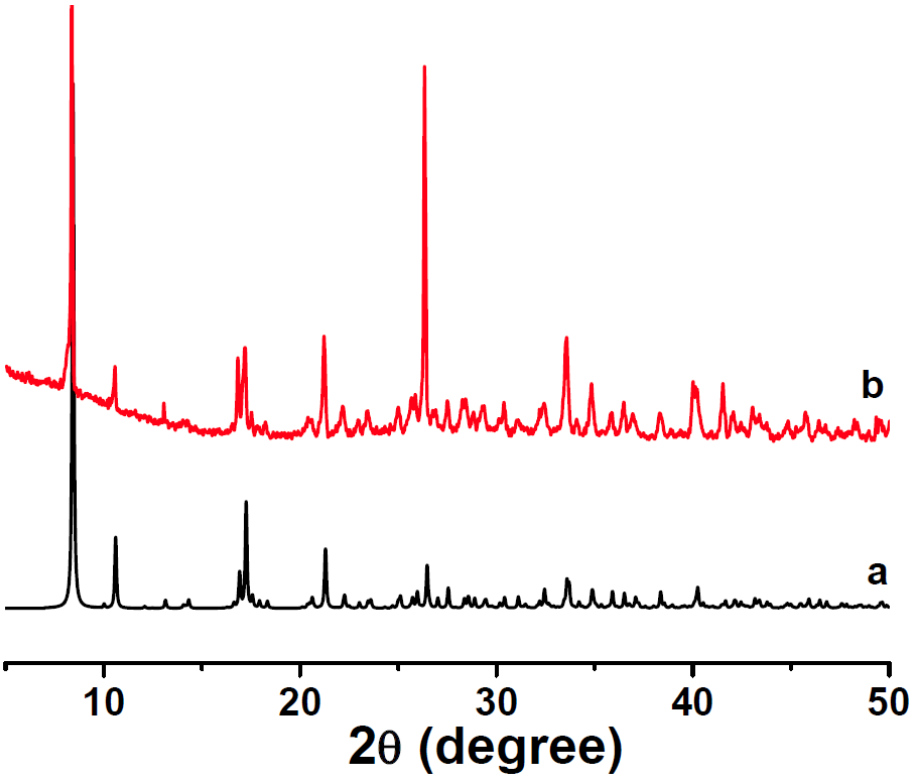

Fig. S5 PXRD patterns for **4**. (a) simulated; (b) a single-phase polycrystalline sample of **4**.

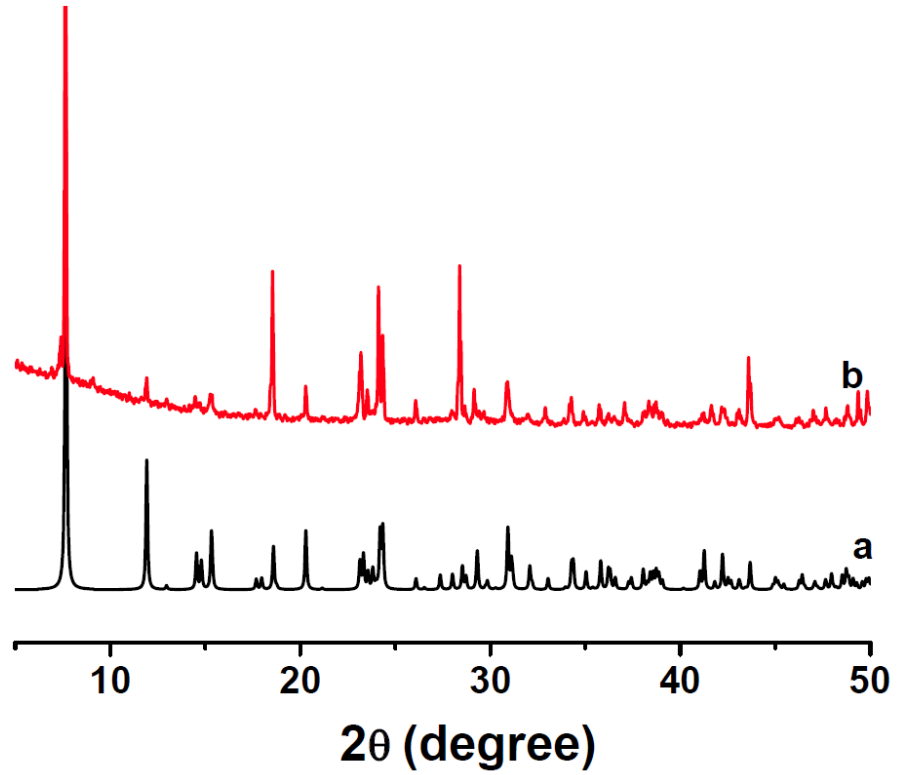

Fig. S6 PXRD patterns for **5**. (a) simulated; (b) a single-phase polycrystalline sample of **5**.

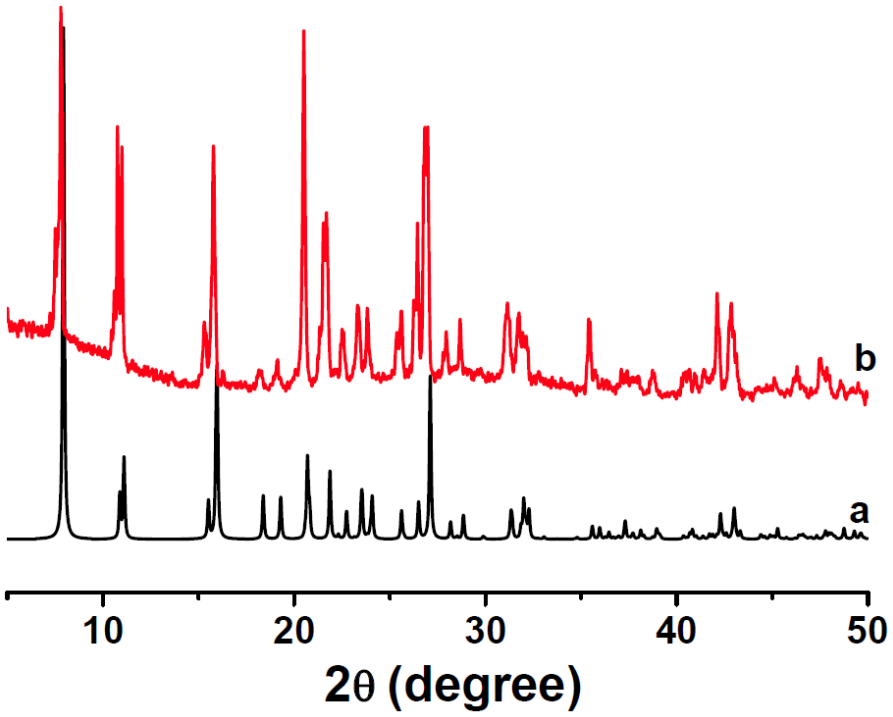

Fig. S7 PXRD patterns for $[(5\text{-phpyms})_2Cu]_n$. (a) simulated; (b) a single-phase polycrystalline sample of $[(5\text{-phpyms})_2Cu]_n$.

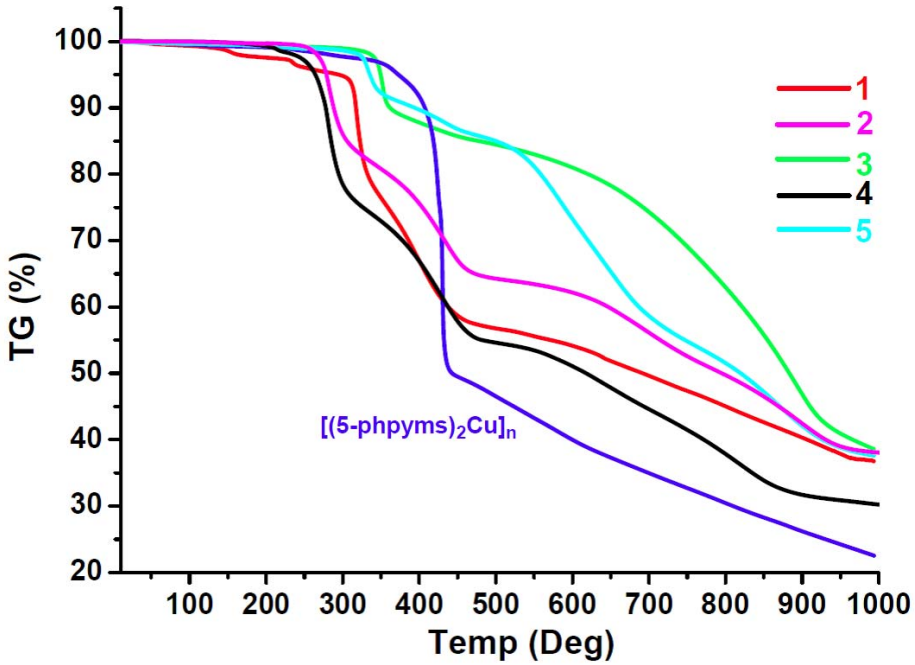

Fig. S8 TGA curves of **1-5** and $[(5\text{-phpyms})_2Cu]_n$.

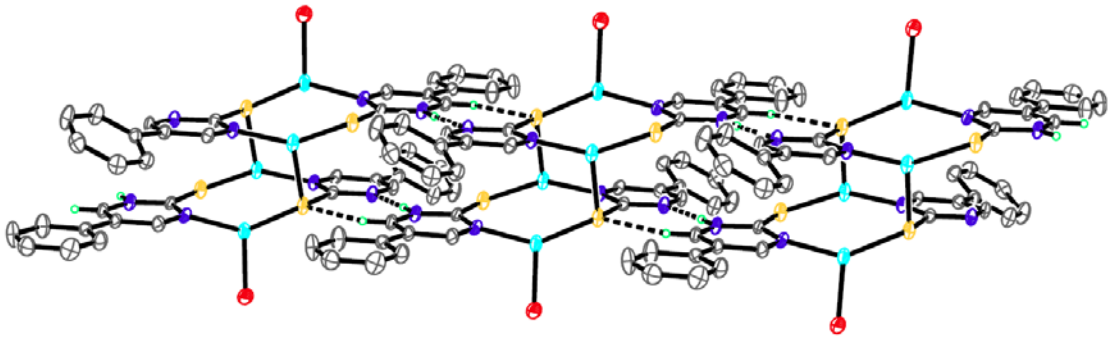

Fig. S9 View of the 1D hydrogen-bound structure of **2**.

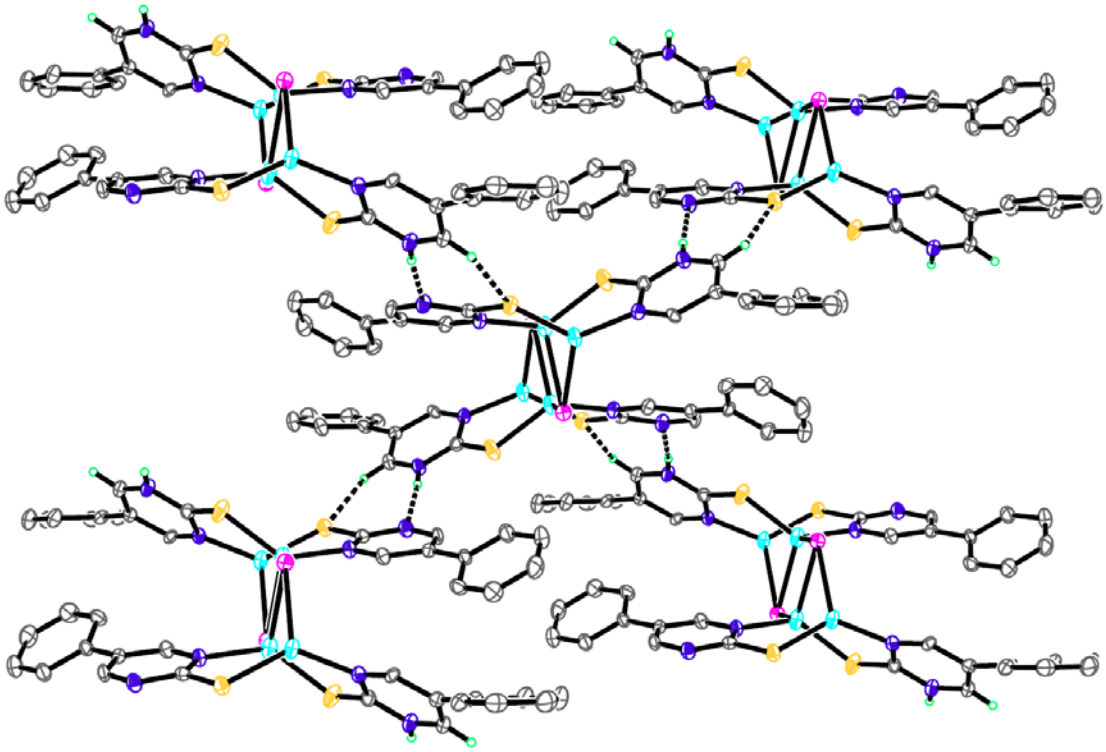

Fig. S10 View of the 2D hydrogen-bound structure of **4**.

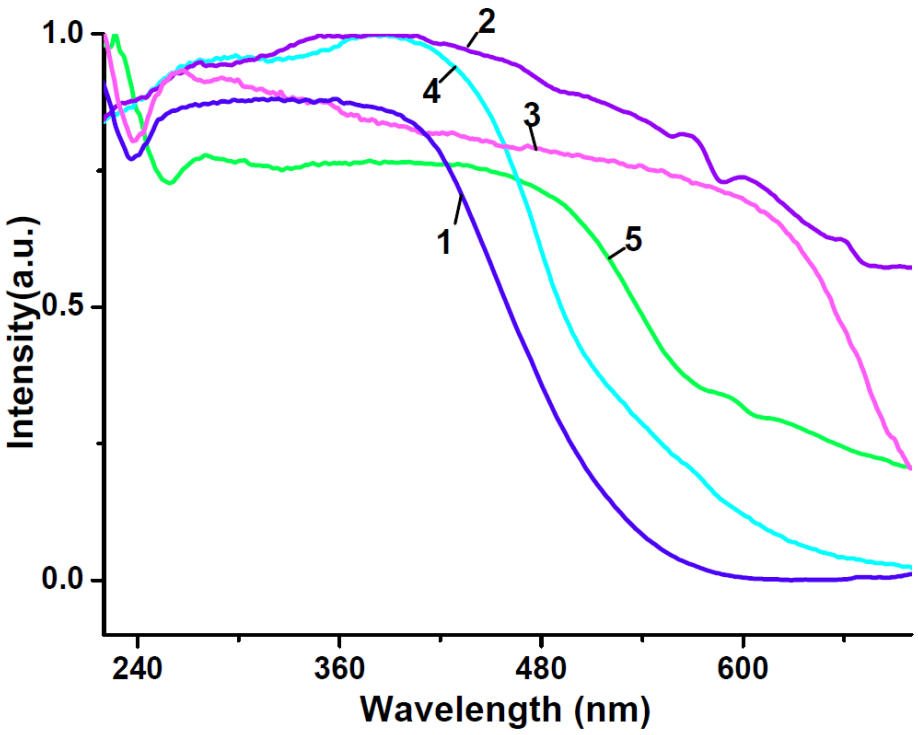

Fig. S11 The UV−vis spectra of complexes **1-5** in the solid state.

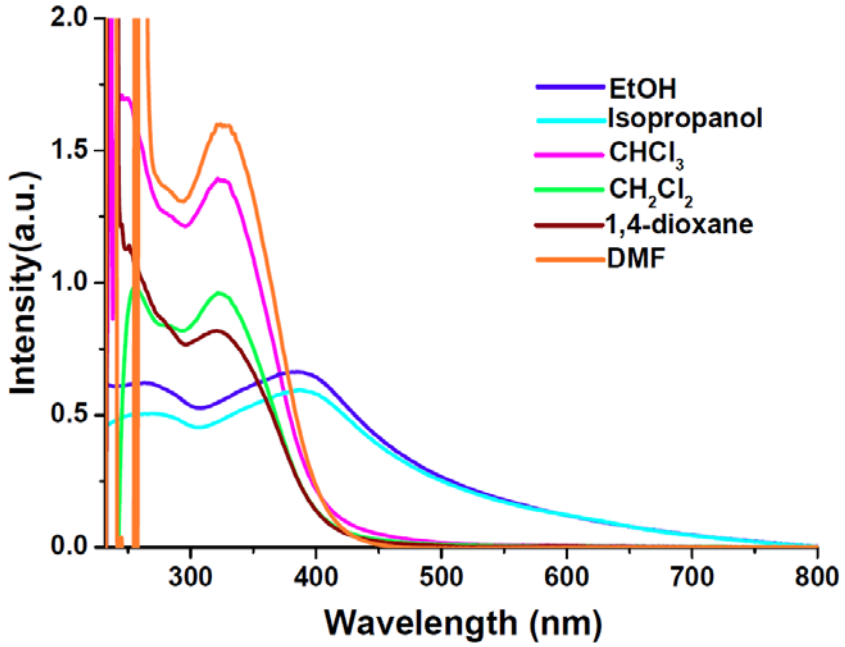

Fig. S12 UV-Vis absorption spectra of **1** in various solvents (1×10^{-4} mol/L)

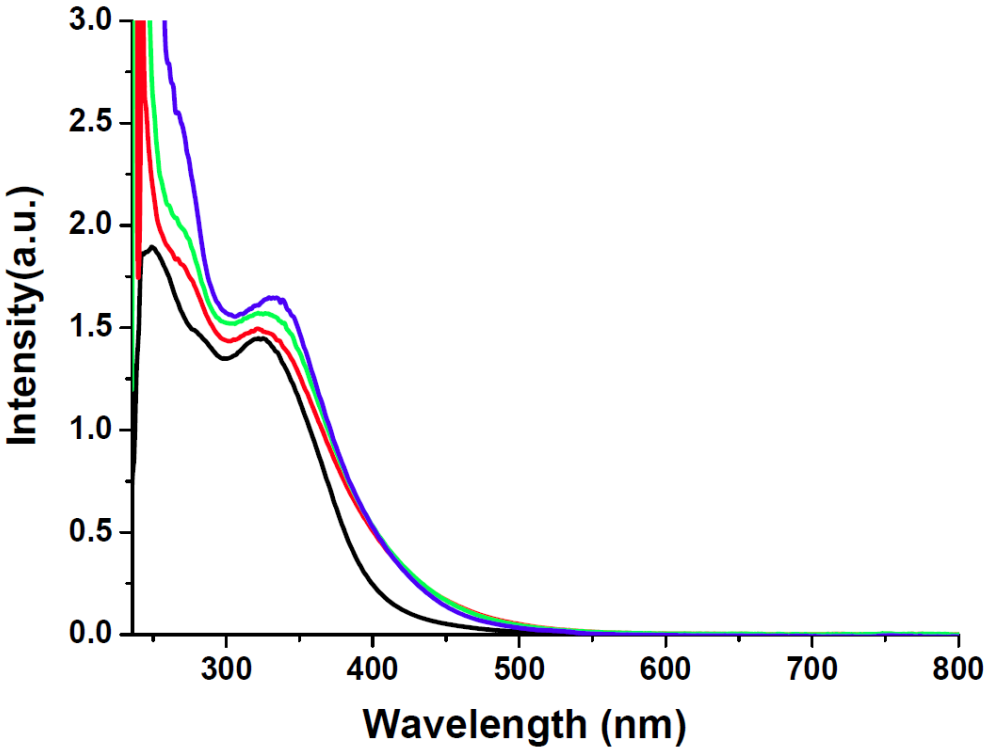

Fig. S13 UV-Vis absorption spectra of **1** in $CHCl_3$, black (1×10^{-4} mol/L), red ($c_{CF3COOH} = 10^{-2}$ mol/L), green ($c_{CF3COOH} = 10^{-1}$ mol/L) and blue ($c_{CF3COOH} = 5 \times 10^{-1}$ mol/L).

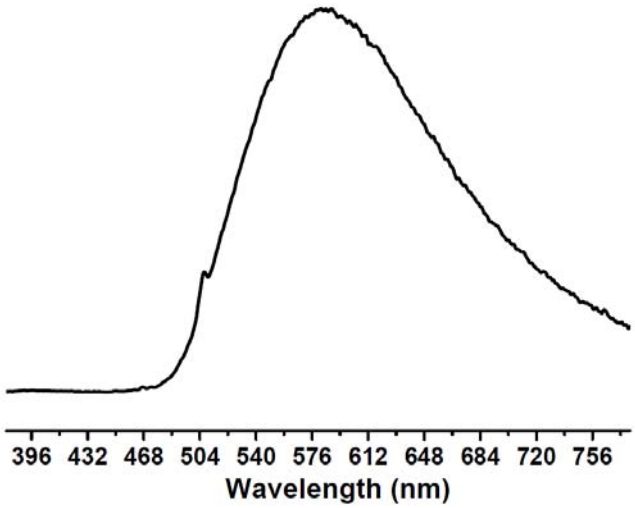

Fig. S14 Emission spectrum of **1** in the solid state at room temperature.

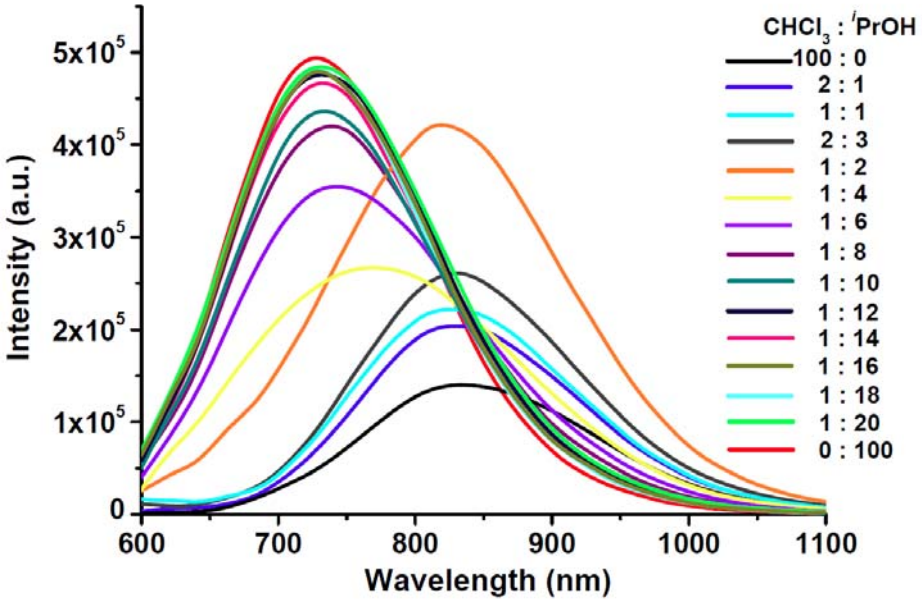

Fig. S15 Emission spectra of **1** (1×10^{-6} mol/L) in $CHCl_3$/isopropanol mixture.

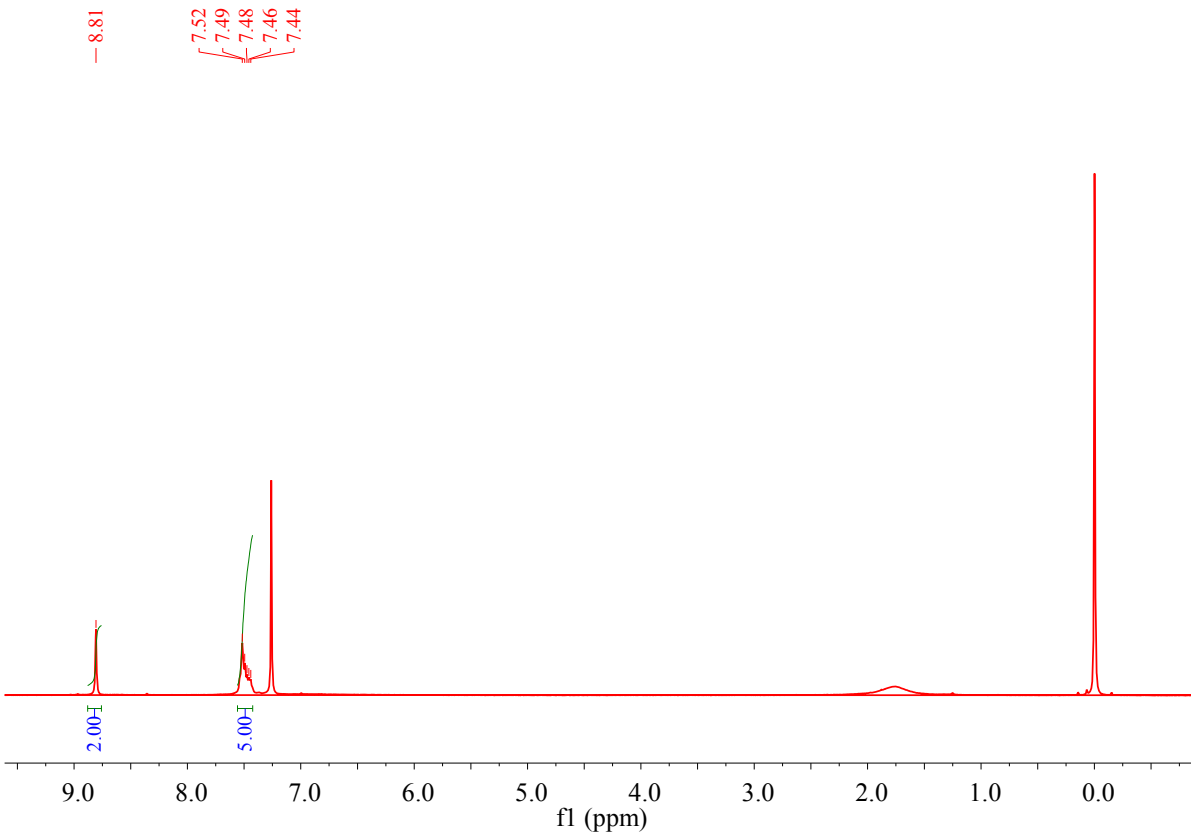

Fig. S16 ^{1}H NMR spectrum of **1**

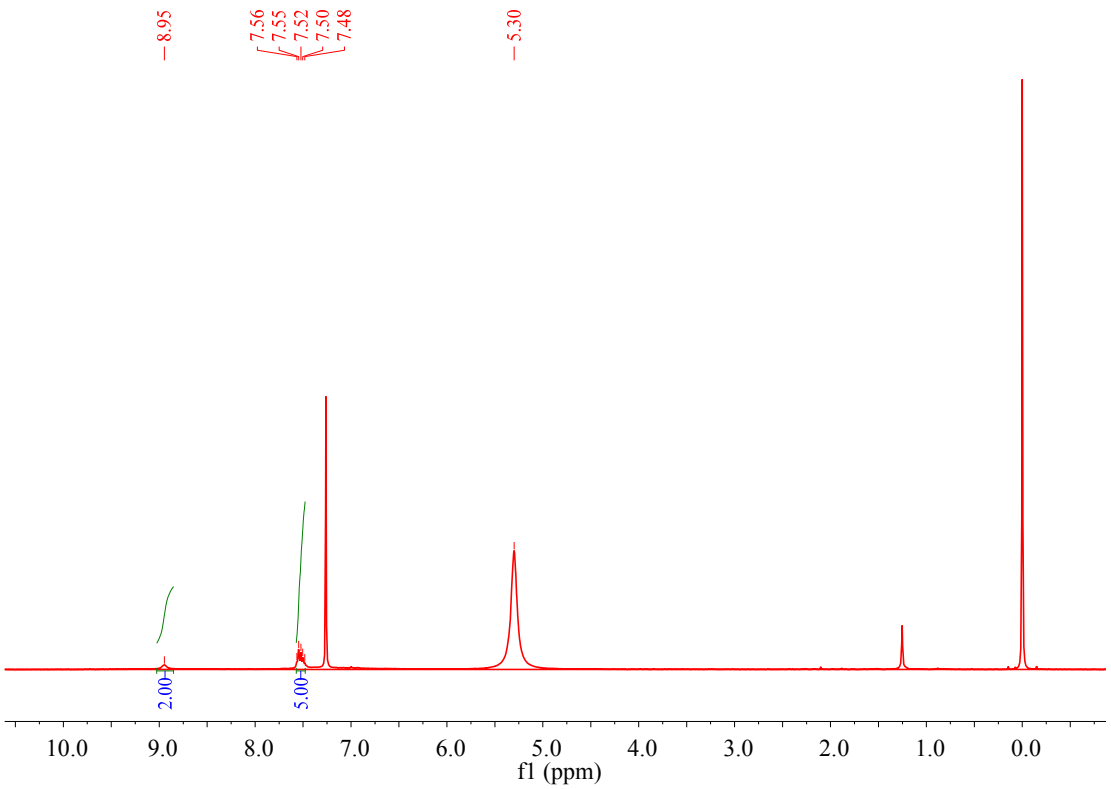

Fig. S17 ^{1}H NMR spectrum of **1**with CF_3COOH.

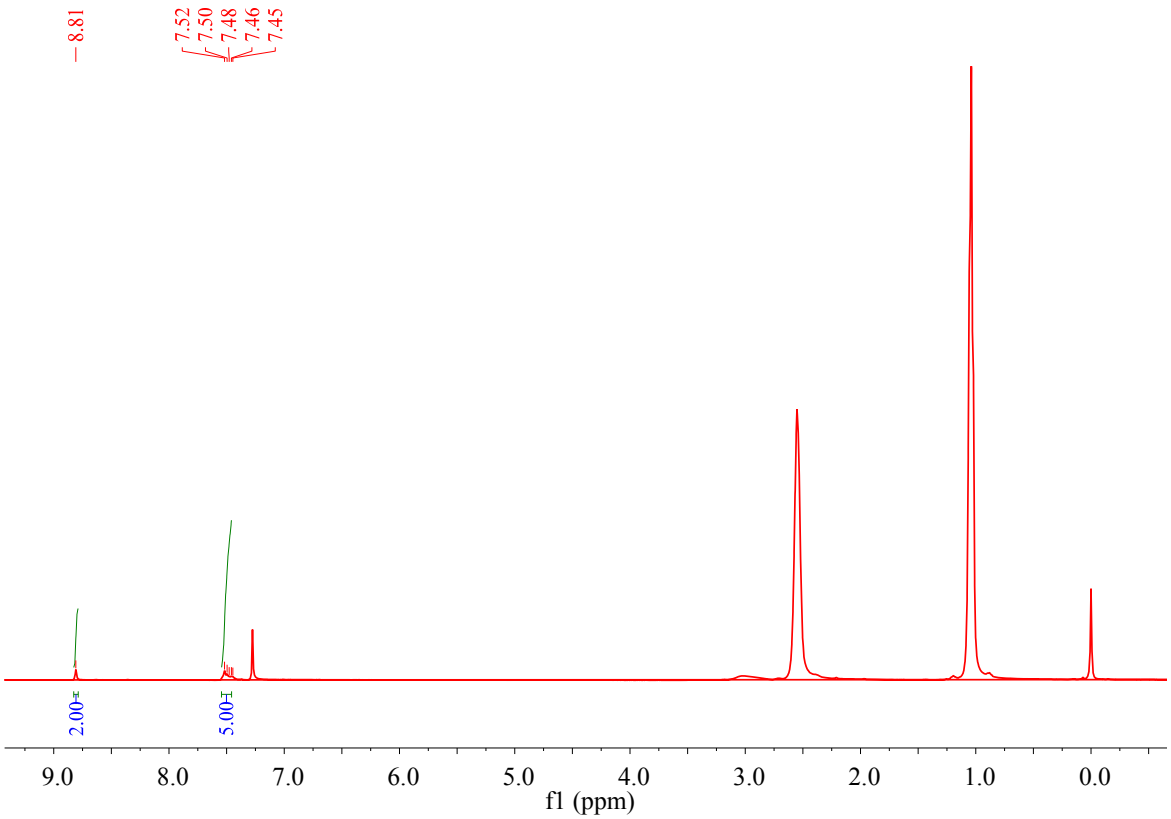

Fig. S18 ^{1}H NMR spectrum of **1** after the addition of CF_3COOH and then Et_3N.

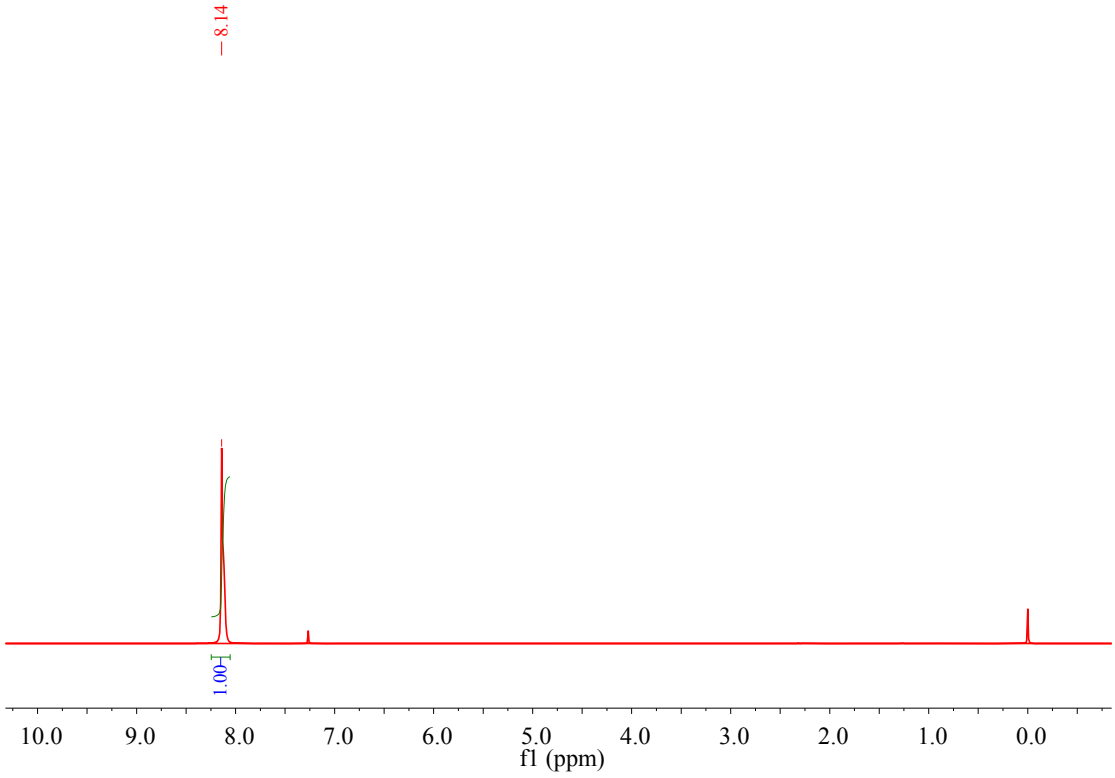

Fig. S19 ^{1}H NMR spectrum of CF_3COOH.

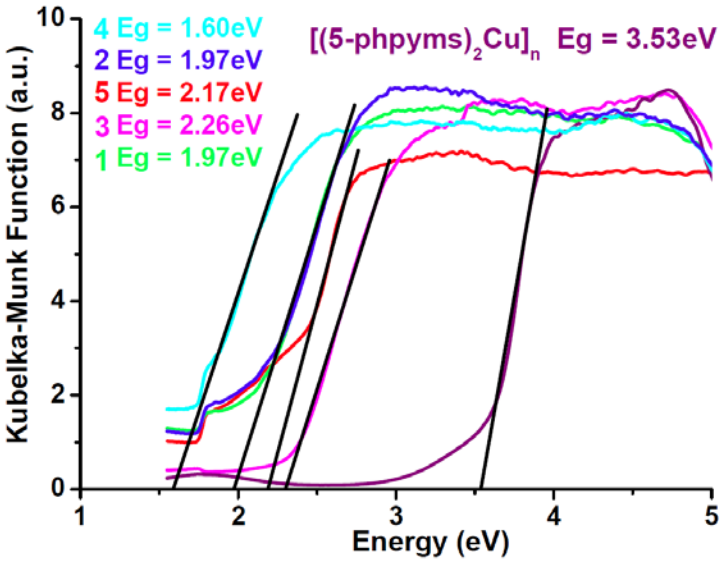

Fig. S20 Solid-state optical diffuse-reflection spectra of **1**-**5** and $[(5\text{-phpyms})_2Cu]_n$ with $BaSO_4$ as background derived from the diffuse reflectance data at ambient temperature.

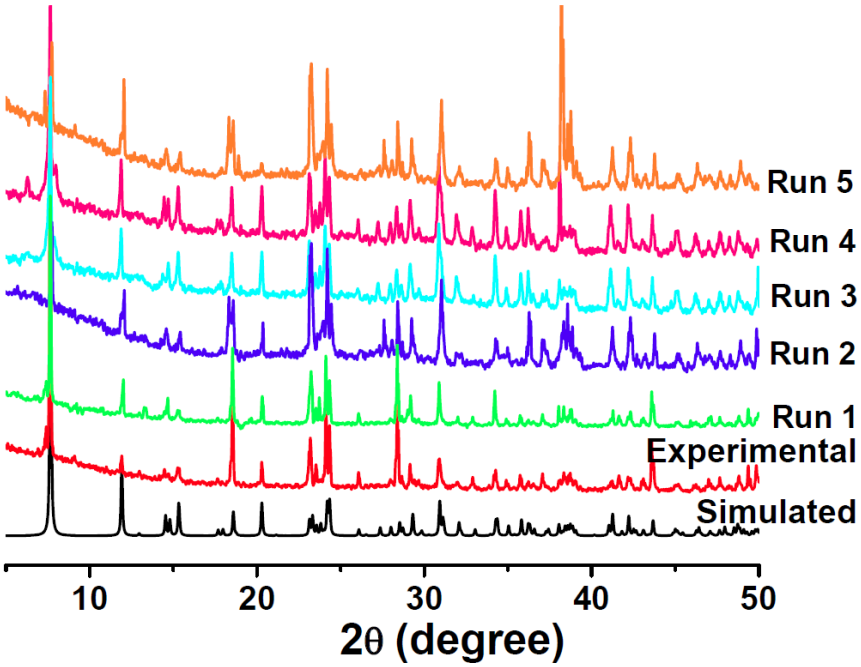

Fig. S21 PXRD patterns of the simulated, experimental and those after different catalytic cycles of compound **5**.

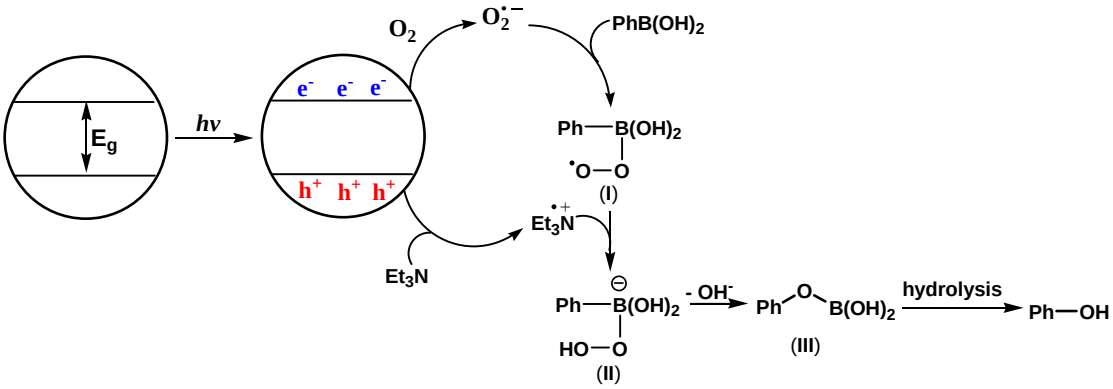

Scheme S1 Proposed mechanism for the oxidative hydroxylation of arylboronic acids.

^{1}H and ^{13}CNMR data of the phenols

Phenol

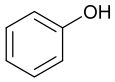

^{1}H NMR (400 MHz, DMSO-d_6) δ 9.32 (s, 1H), 7.36 - 7.02 (m, 2H), 6.75 (d, *J* = 7.5 Hz, 3H). ^{13}C NMR (101 MHz, DMSO-d_6) δ 157.20, 129.10, 118.68, 114.77.

4-methoxyphenol

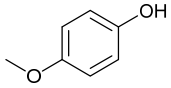

^{1}H NMR (400 MHz, DMSO-d_6) δ 8.88 (s, 1H), 6.74 (d, *J* = 8.7 Hz, 2H), 6.67 (d, *J* = 8.6 Hz, 2H), 3.65 (s, 3H). ^{13}C NMR (151 MHz, DMSO-d_6) δ 151.98, 151.09, 115.69, 114.39, 55.31.

4-methylphenol

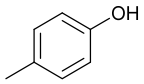

^{1}H NMR (400 MHz, DMSO-d_6) δ 9.06 (s, 1H), 6.95 (d, *J* = 7.9 Hz, 2H), 6.64 (d, *J* = 8.1 Hz, 2H), 2.17 (s, 3H). ^{13}C NMR (101 MHz, DMSO-d_6) δ 154.55, 129.75, 127.17, 114.76, 19.96.

3-methoxyphenol

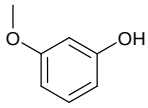

^{1}H NMR (400 MHz, DMSO-d_6) δ 9.41 (s, 1H), 7.06 (t, *J* = 7.9 Hz, 1H), 6.39 (t, *J* = 11.1 Hz, 3H), 3.69 (s, 3H). ^{13}C NMR (151 MHz, DMSO-d_6) δ 160.7, 158.8, 130.0, 108.0, 104.7, 101.4, 54.9.

3-methylphenol

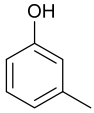

^{1}H NMR (400 MHz, DMSO-d_6) δ 9.98 (s, 1H), 7.51 (d, *J* = 6.2 Hz, 2H), 7.41 (s, 1H), 7.30 - 7.25 (m, 1H), 3.82 (s, 3H). ^{13}C NMR (101 MHz, DMSO-d_6) δ 157.45, 138.48, 129.30, 119.86, 116.26, 112.71, 21.17.

2-methoxyphenol

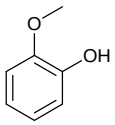

^{1}H NMR (400 MHz, DMSO-d_6) δ 8.90 (s, 1H), 6.92 – 6.87 (m, 1H), 6.80 – 6.71 (m, 3H), 3.75 (s, 3H). ^{13}C NMR (151 MHz, DMSO-d_6) δ 147.7, 146.6, 120.9, 119.3, 115.6, 112.4, 55.6

2-methylphenol

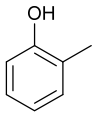

^{1}H NMR (400 MHz, DMSO-d_6) δ 9.24 (s, 1H), 7.11 - 6.96 (m, 2H), 6.85 (s, 1H), 6.70 (d, *J* = 6.0 Hz, 1H), 2.18 (s, 3H). ^{13}C NMR (101 MHz, DMSO-d_6) δ 155.51, 130.63, 126.68, 123.89, 118.86, 114.70, 16.06.

2,6-dimethylphenol

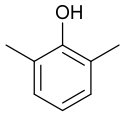

^{1}H NMR (400 MHz, DMSO-d_6) δ 8.17 (s, 1H), 6.90 (d, *J* = 7.4 Hz, 2H), 6.64 (t, *J* = 7.4 Hz, 1H), 2.10 (s, 6H). ^{13}C NMR (151 MHz, DMSO-d_6) δ 152.97, 127.89, 124.27, 119.14, 16.48.

2,4,6-trimethylphenol

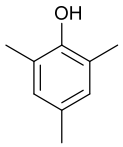

^{1}H NMR (400 MHz, DMSO-d_6) δ 7.89 (s, 1H), 6.69 (s, 2H), 2.11 (s, 9H). ^{13}C NMR (151 MHz, DMSO-d_6) δ 150.75, 128.79, 127.47, 123.97, 19.66, 16.06.

4-nitrophenol

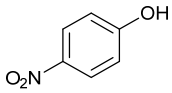

^{1}H NMR (400 MHz, DMSO-d_6) δ 11.03 (s, 1H), 8.11 (d, *J* = 7.8 Hz, 2H), 6.92 (d, *J* = 8.5 Hz, 2H). ^{13}C NMR (151 MHz, DMSO-d_6) δ 163.89, 139.61, 126.16, 115.77.

4-acetylphenol

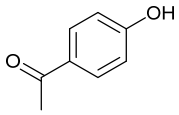

^{1}H NMR (400 MHz, DMSO-d_6) δ 10.34 (s, 1H), 7.84 (d, *J* = 8.2 Hz, 2H), 6.85 (d, *J* = 8.2 Hz, 2H), 2.47 (s, 3H). ^{13}C NMR (151 MHz, DMSO-d_6) δ 195.75, 161.79, 130.69, 128.49, 115.13, 25.86.

4-fluorophenol

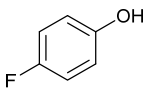

^{1}H NMR (400 MHz, DMSO-d_6) δ 9.34 (s, 1H), 7.00–6.94 (m, 2H), 6.76–6.71 (m, 2H). ^{13}C NMR (101 MHz, DMSO-d_6) δ 156.7, 154.3, 153.6 (d), 116.1 (d), 115.7, 115.5.

2-naphthylphenol

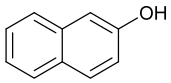

^{1}H NMR (400 MHz, DMSO-d_6) δ 9.71 (s, 1H), 7.78 - 7.72 (m, 2H), 7.67 (d, *J* = 8.2 Hz, 1H), 7.38 (t, *J* = 7.4 Hz, 1H), 7.25 (t, *J* = 7.4 Hz, 1H), 7.12 - 7.05 (m, 2H). ^{13}C NMR (101 MHz, DMSO-d_6) δ 155.25, 134.57, 129.26, 127.70, 127.51, 126.07, 125.95, 122.60, 118.58, 108.61.

hydroquinone

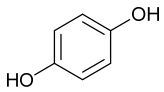

^{1}H NMR (400 MHz, DMSO-d_6) δ 8.61 (s, 2H), 6.55 (s, 4H). ^{13}C NMR (101 MHz, DMSO-d_6) δ 149.73, 115.46.

m-dihydroxybenzene

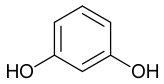

^{1}H NMR (400 MHz, DMSO-d_6) δ 9.14 (s, 2H), 6.91 (t, *J* = 7.8 Hz, 1H), 6.18 (d, *J* = 7.7 Hz, 3H). ^{13}C NMR (151 MHz, DMSO-d_6) δ 158.4, 129.7, 106.2, 102.5.

4-ethylphenol

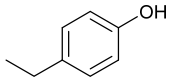

^{1}H NMR (400 MHz, DMSO-d_6) δ 9.09 (s, 1H), 6.98 (t, *J* = 5.6 Hz, 2H), 6.67 (dd, *J* = 6.5, 2.0 Hz, 2H), 2.47 (t, *J* = 7.6 Hz, 2H), 1.12 (t, *J* = 7.6 Hz, 3H). ^{13}C NMR (101 MHz, DMSO-d_6) δ 155.2, 133.8, 128.5, 115.0, 27.3, 16.0.

References

[S1] G. M. Sheldrick, *Acta Cryst.* **2015**, *C71*, 3.

[S2] Kinoshita, I.; Wright, L. J.; Kubo, S.; Kimura, K.; Sakata, A.; Yano, T.; Miyamoto, R.; Nishioka, T.; Isobe, K. *Dalton Trans.* **2003**, 1993.

[S3] Cai, J. W.; Chen, C. H.; Liao, C. Z.; Yao, J. H.; Hu, X. P.; Chen, X. M. *J. Chem. Soc., Dalton Trans.* **2001**, 1137.

[S4] Mahmoudkhani, A. H.; Shimizu, G. K. H. *Inorg. Chem.* **2007**, *46*, 1593.

Fig. S22 The ^{1}H and ^{13}C NMR spectra for phenol

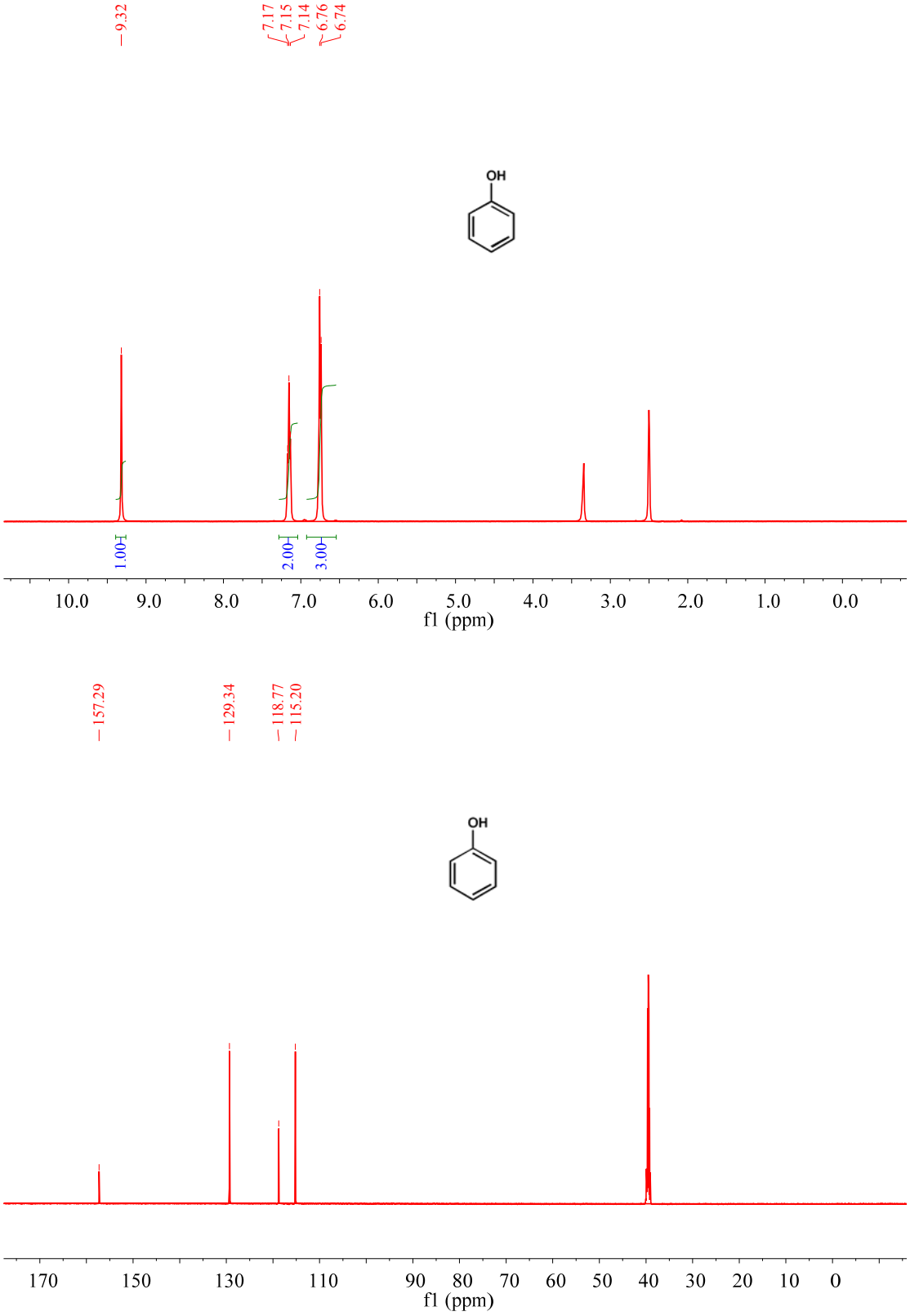

Fig. S23 The ^{1}H and ^{13}C NMR spectra for 4-methoxyphenol

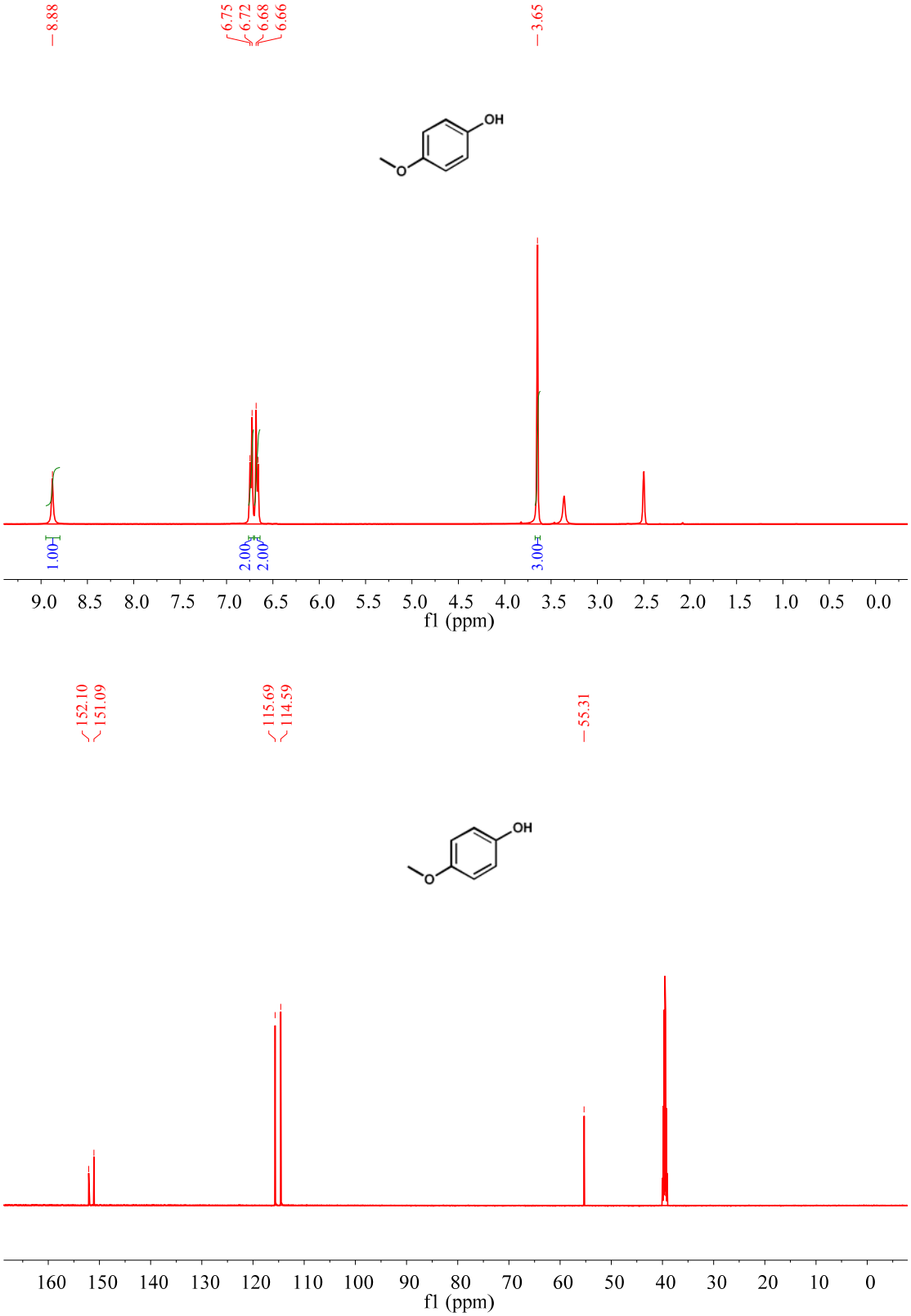

Fig. S24 The ^{1}H and ^{13}C NMR spectra for 4-methylphenol

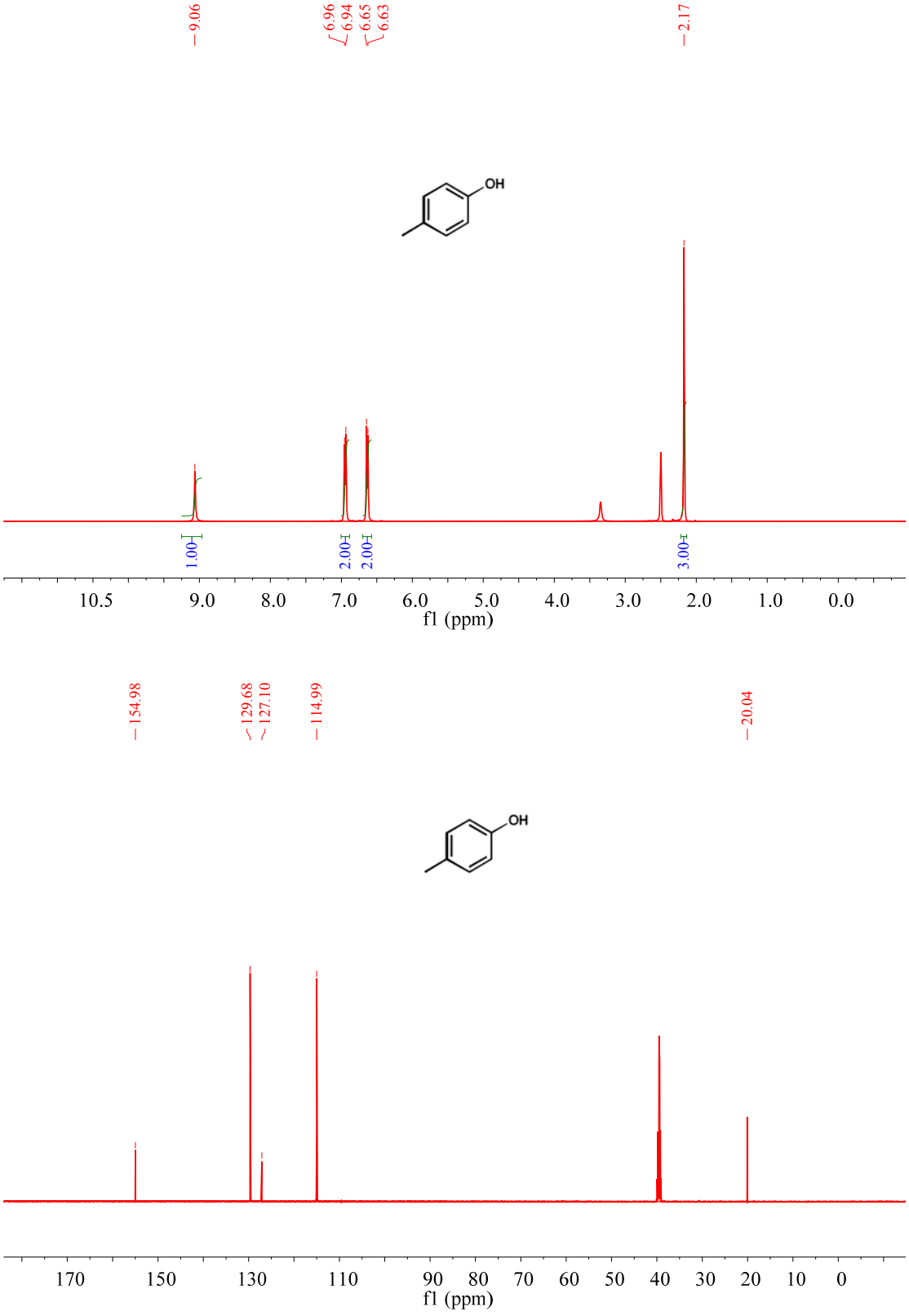

Fig. S25 The ^{1}H and ^{13}C NMR spectra for 3-methoxyphenol

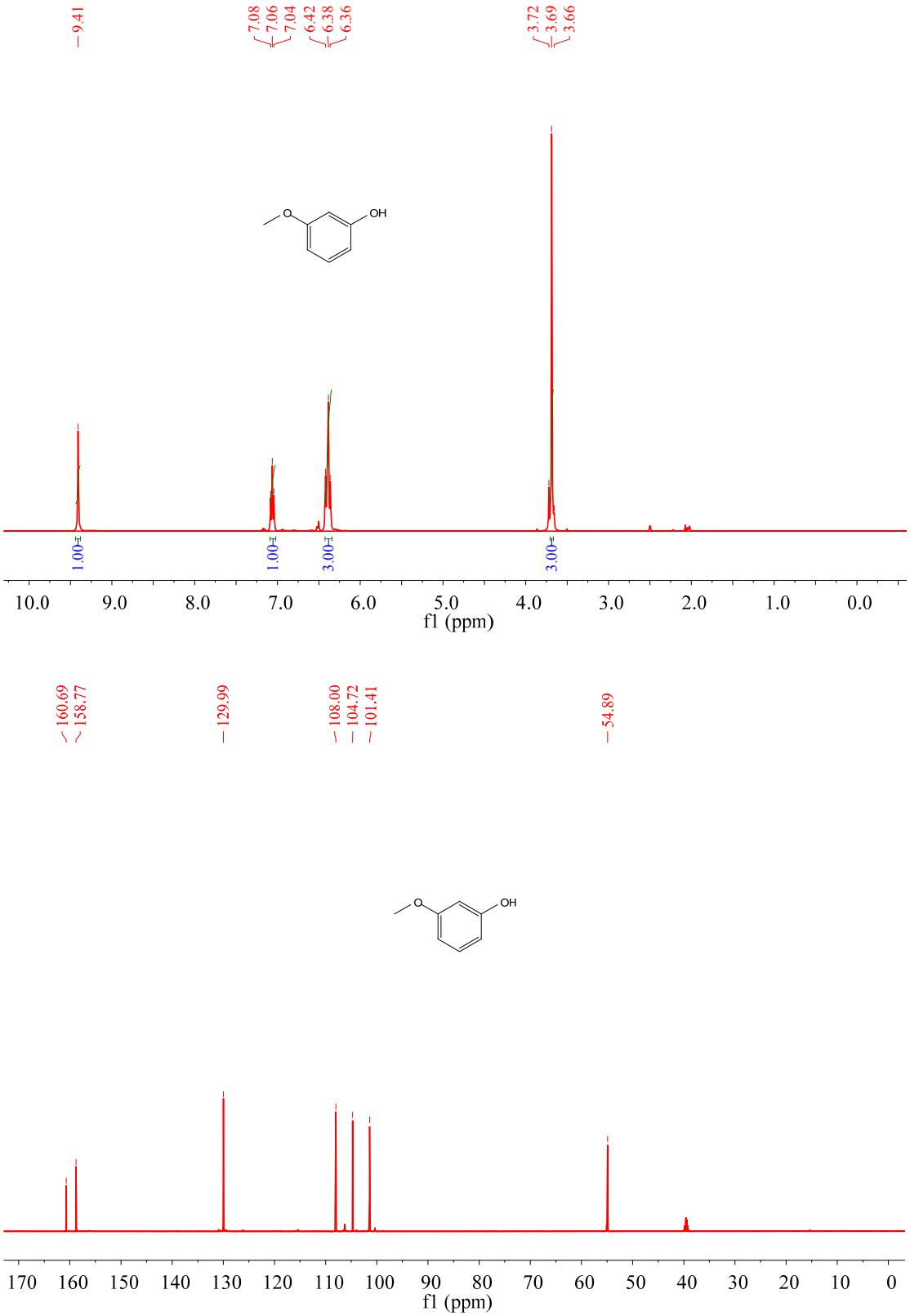

Fig. S26 The ^{1}H and ^{13}C NMR spectra for 3-methylphenol

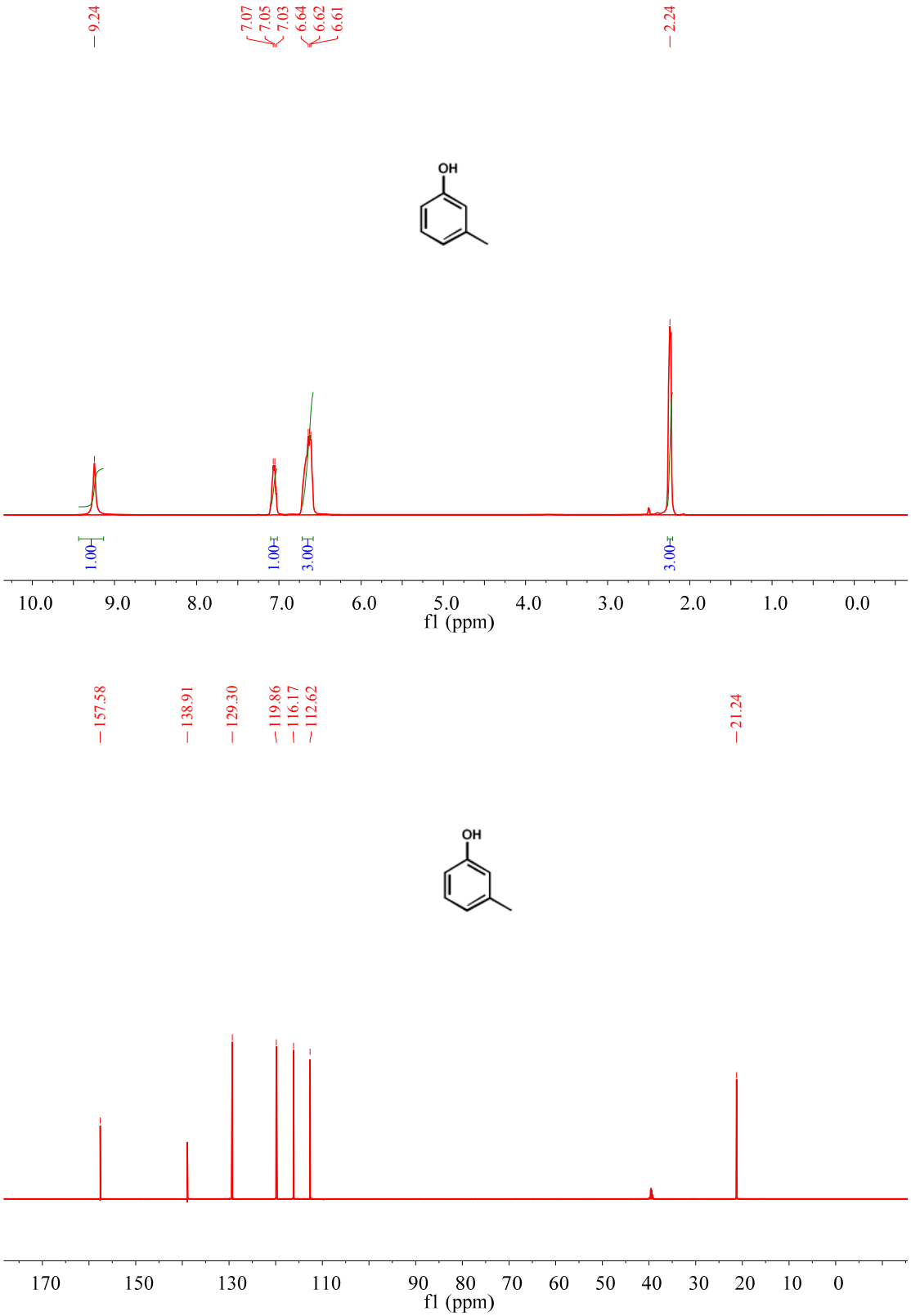

Fig. S27 The ^{1}H and ^{13}C NMR spectra for 2-methoxyphenol

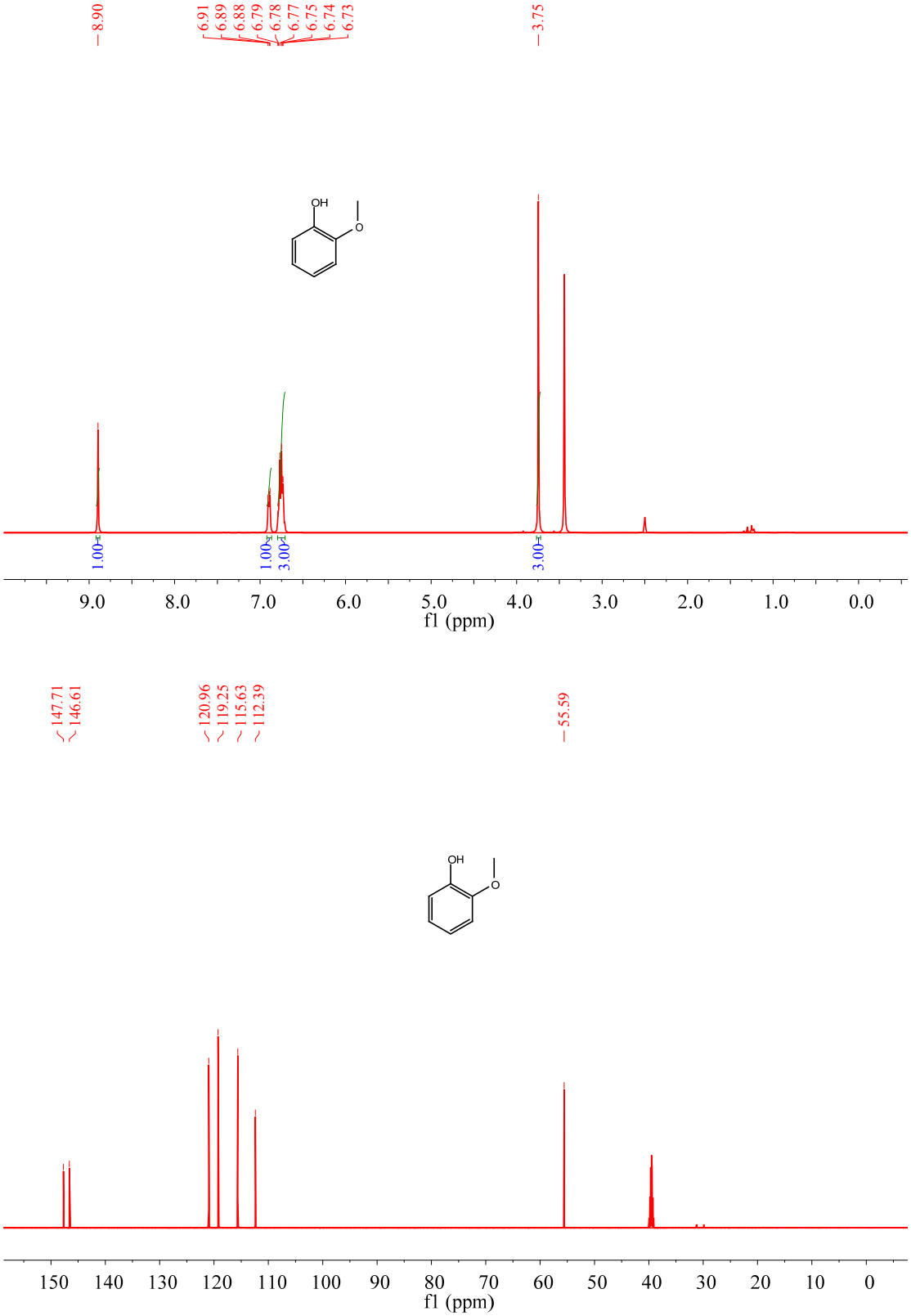

Fig. S28 The ^{1}H and ^{13}C NMR spectra for 2-methylphenol

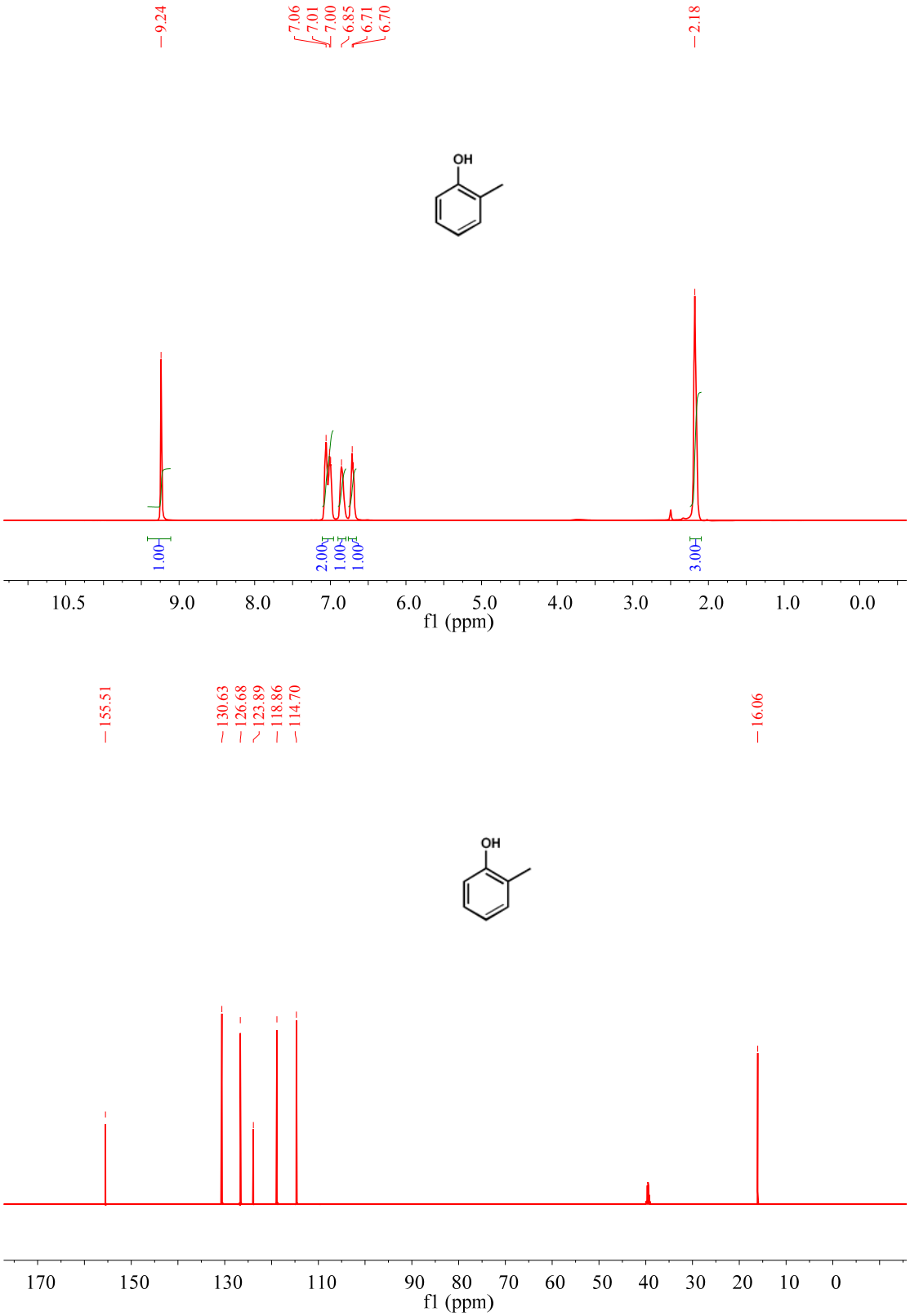

Fig. S29 The ^{1}H and ^{13}C NMR spectra for 2,6-dimethylphenol

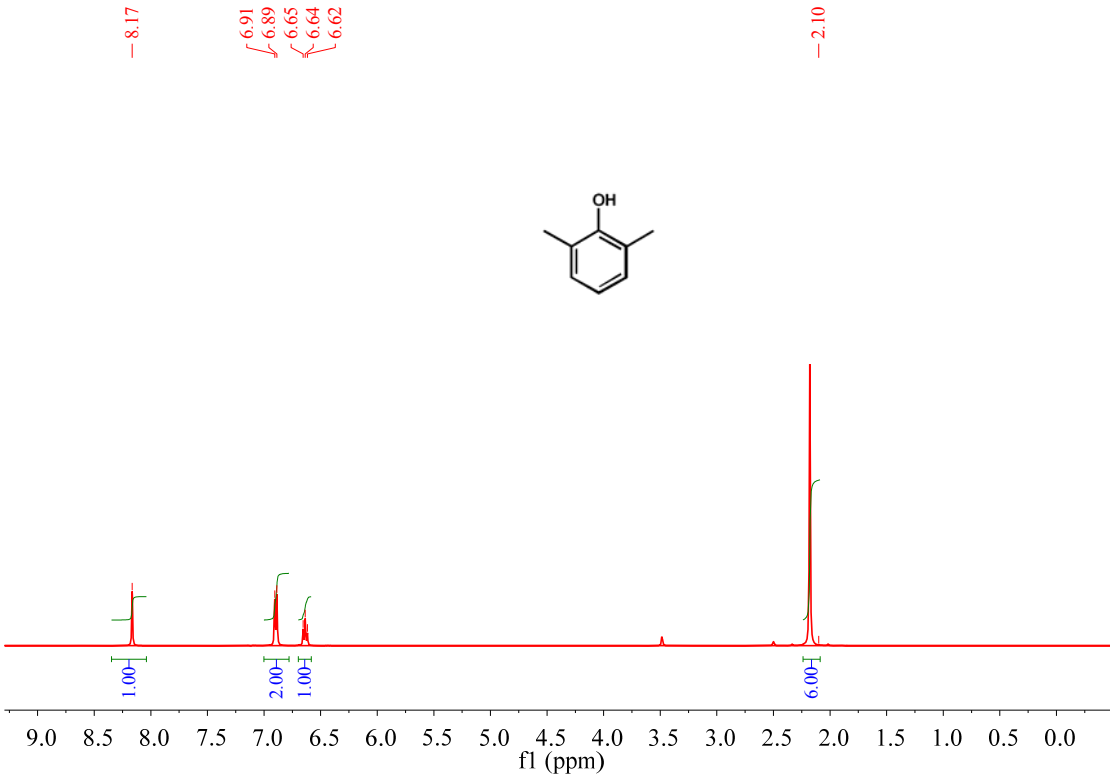

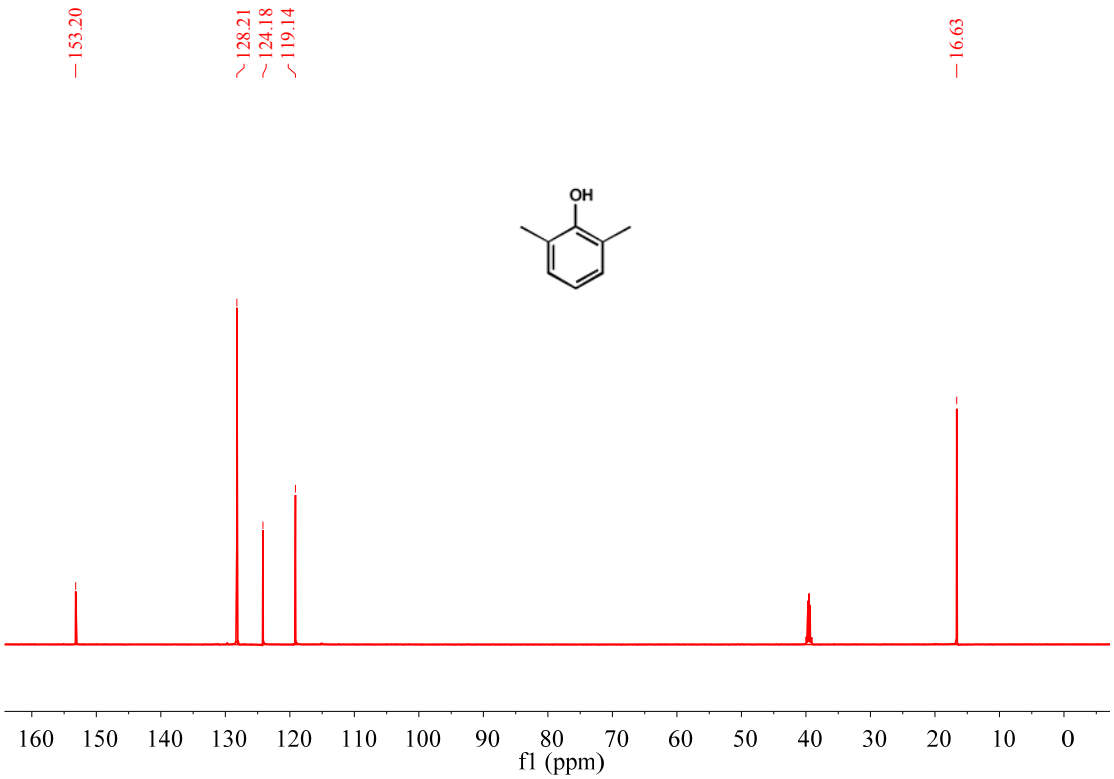

Fig. S30 The ^{1}H and ^{13}C NMR spectra for 2,4,6-trimethylphenol

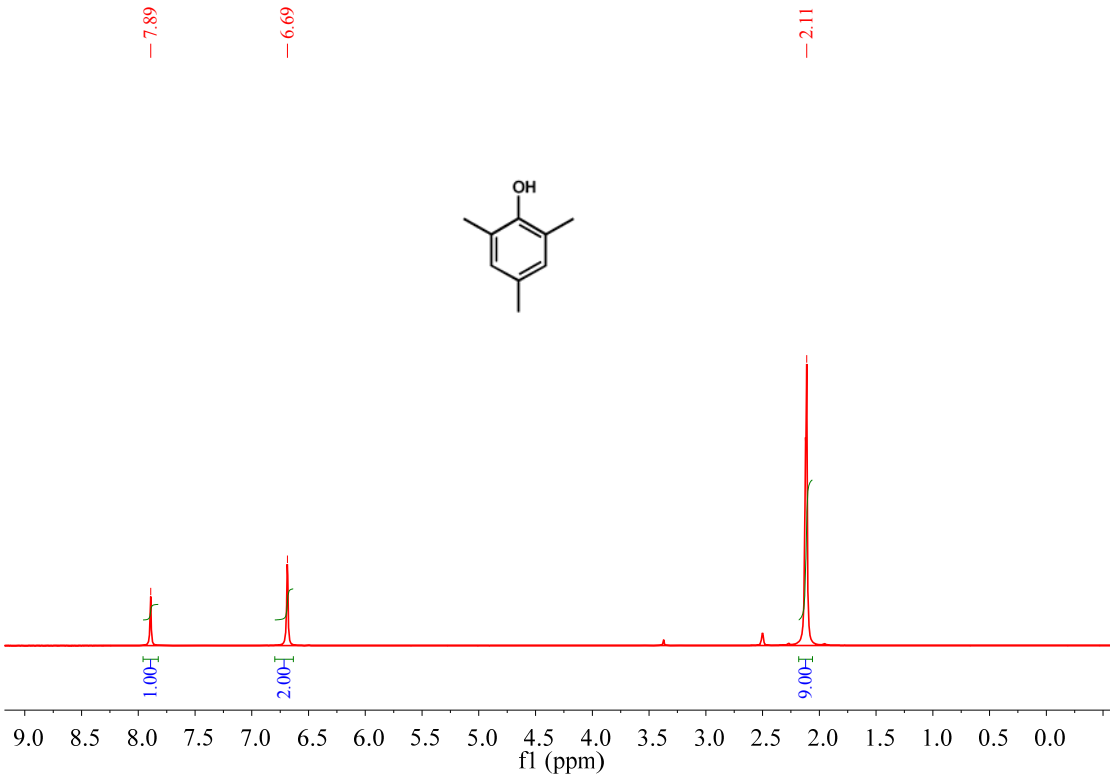

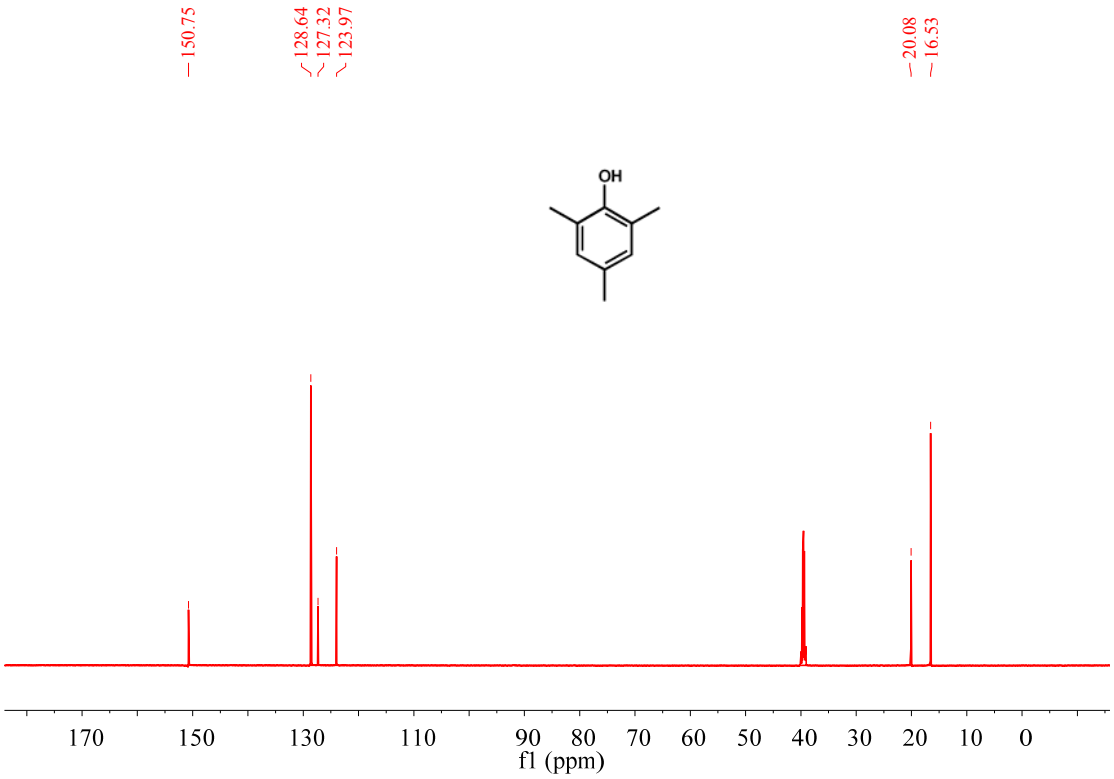

Fig. S31 The ^{1}H and ^{13}C NMR spectra for 4-nitrophenol

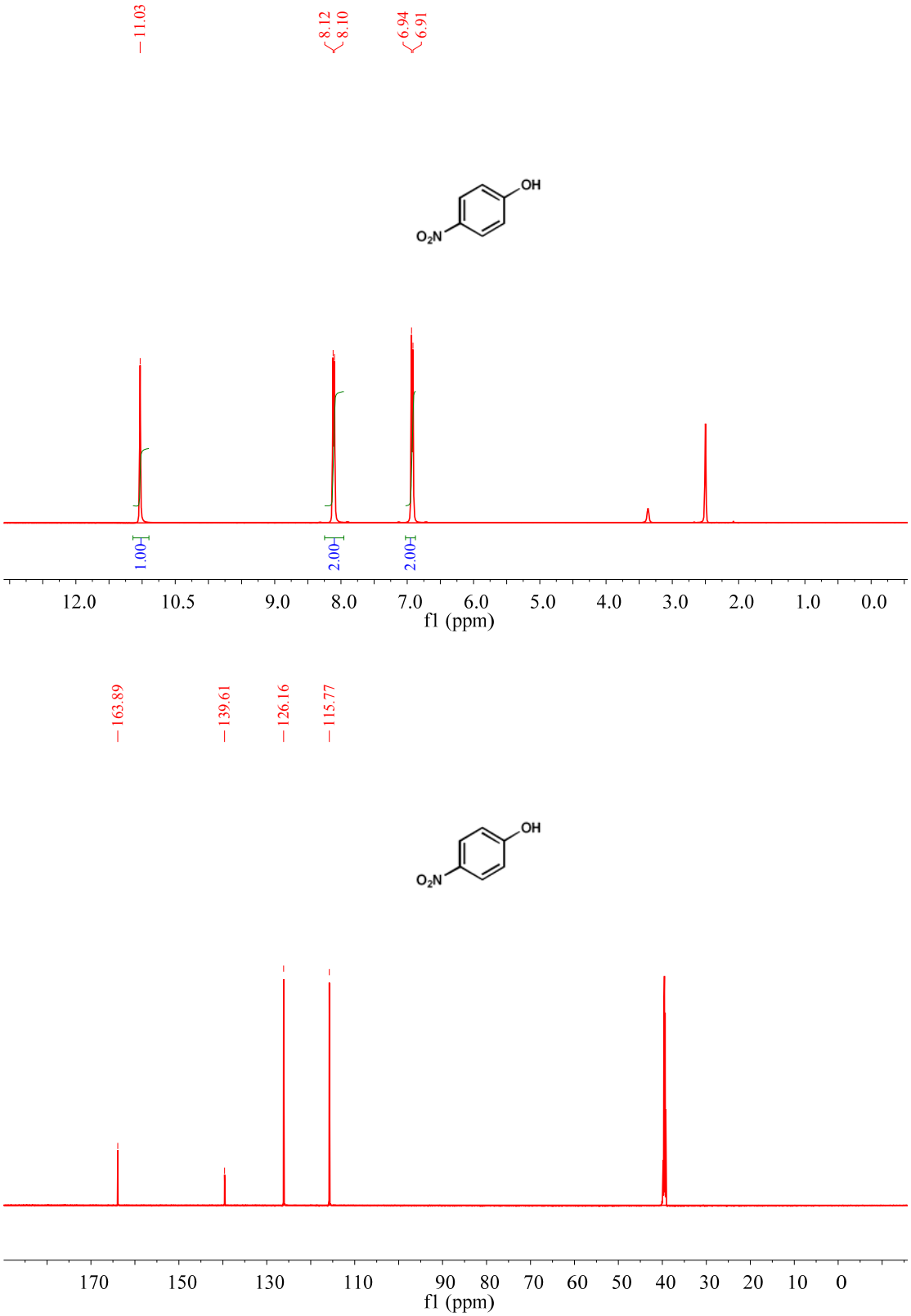

Fig. S32 The ^{1}H and ^{13}C NMR spectra for 4-acetylphenol

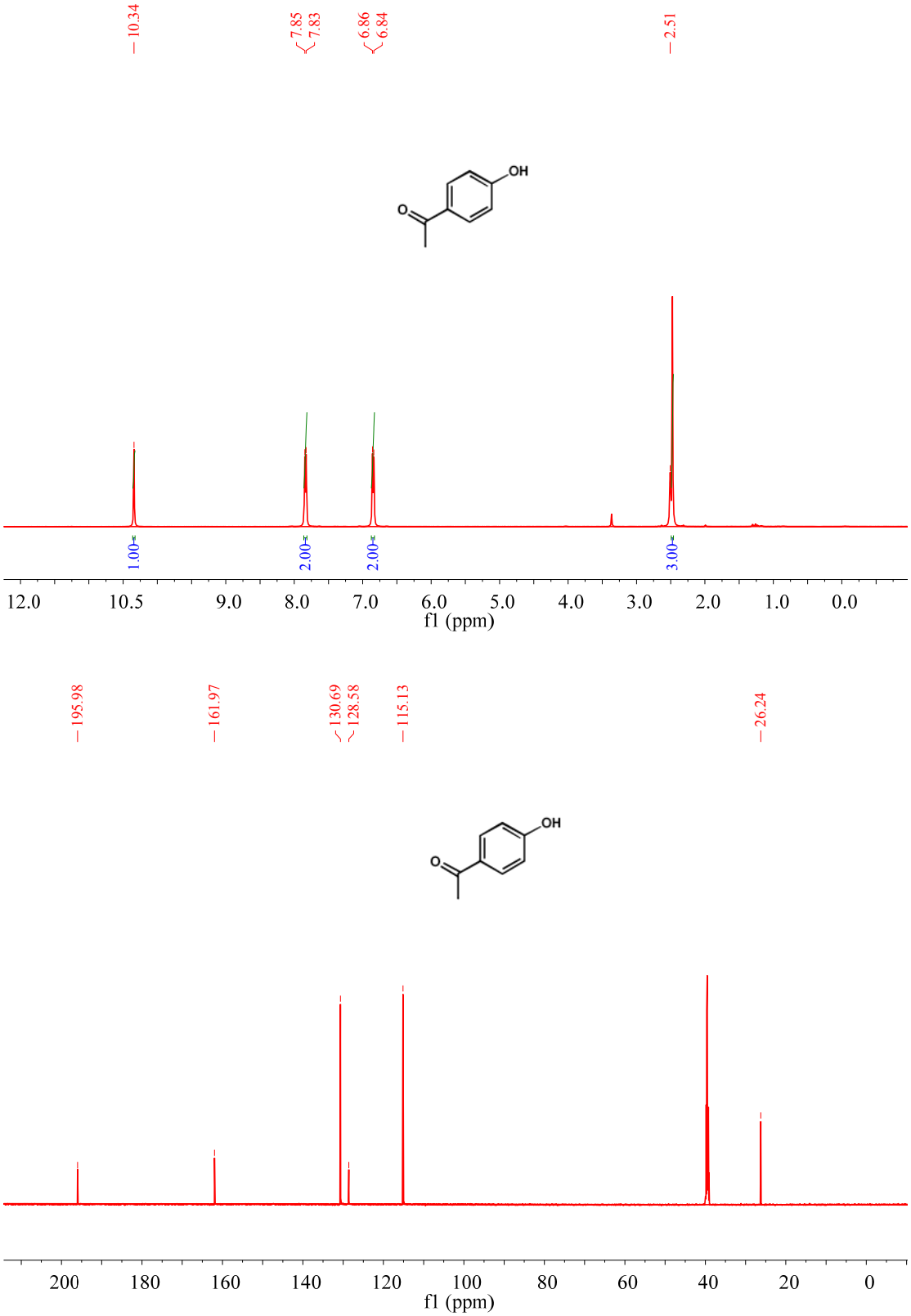

Fig. S33 The ^{1}H and ^{13}C NMR spectra for 4-fluorophenol

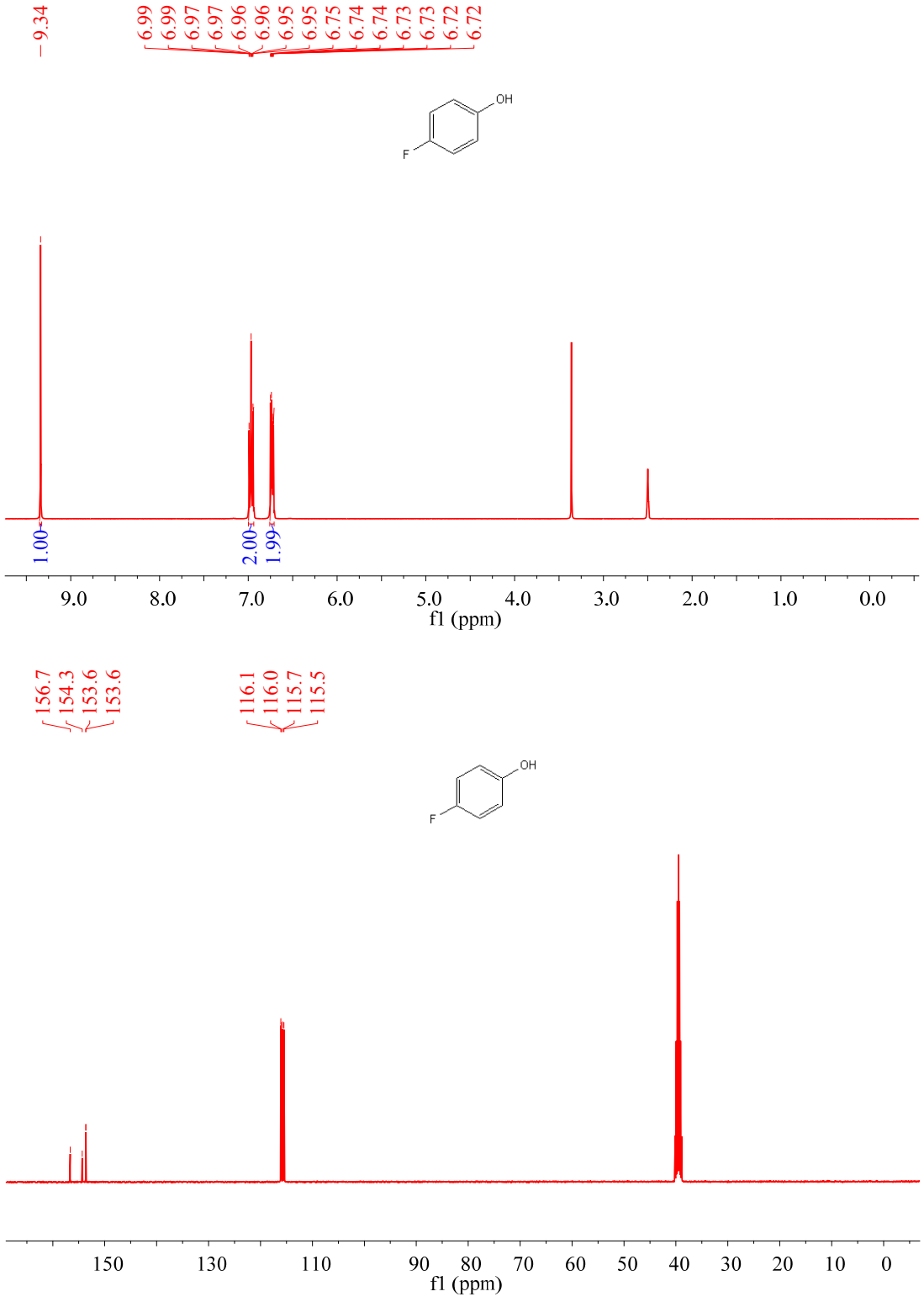

Fig. S34 The ^{1}H and ^{13}C NMR spectra for 2-naphthyphenol

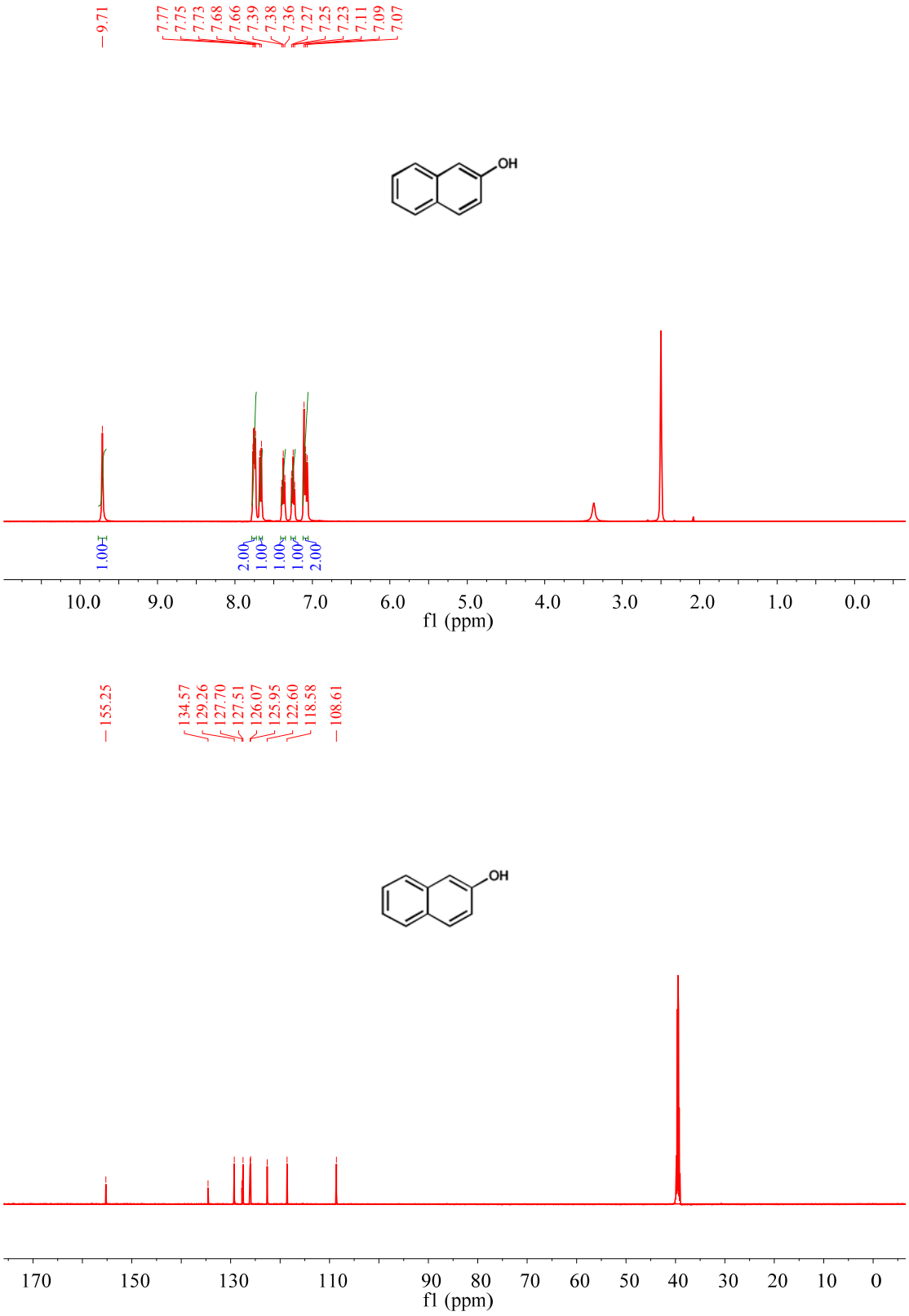

Fig. S35 The ^{1}H and ^{13}C NMR spectra for p-dihydroxybenzene

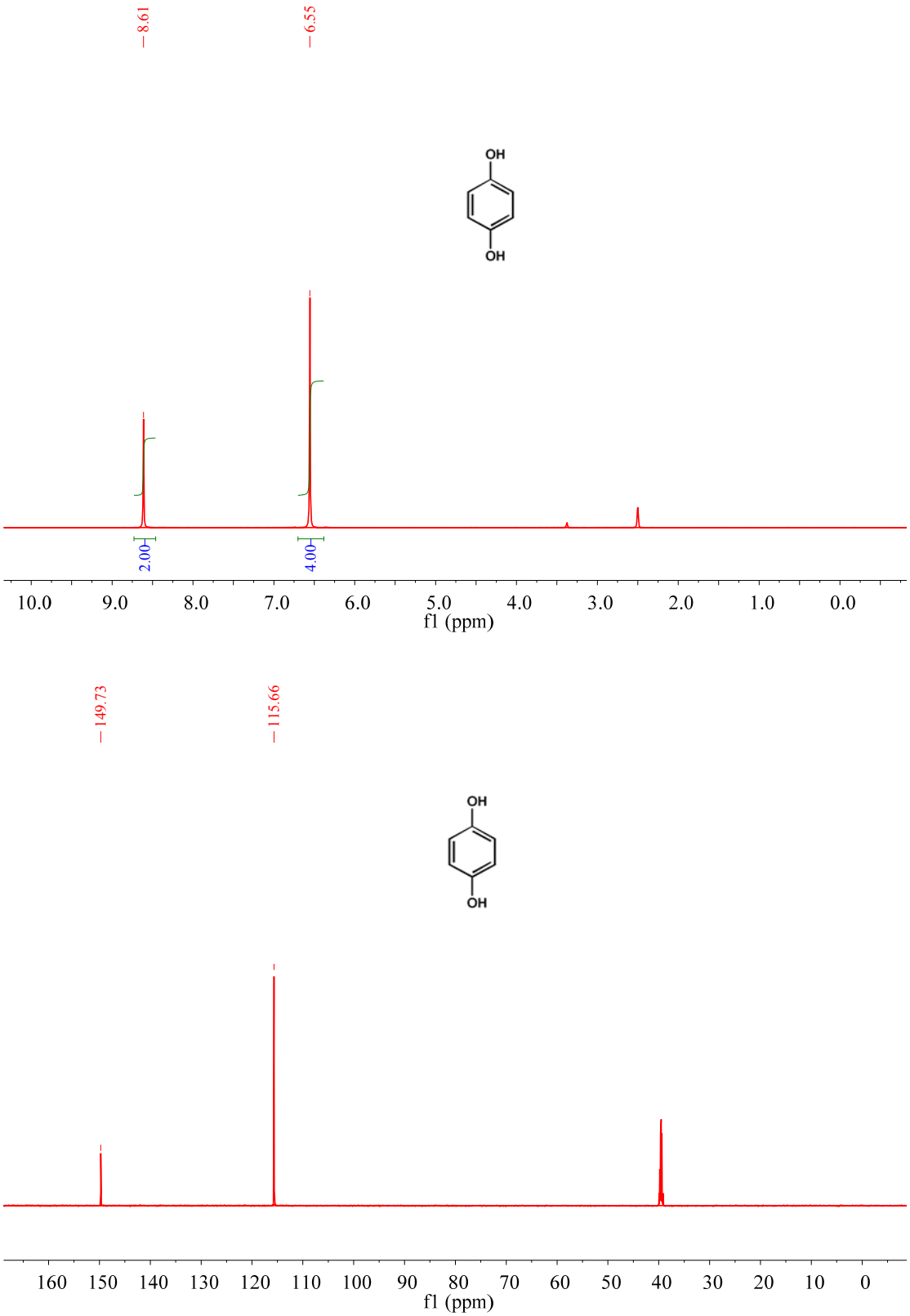

Fig. S36 The ^{1}H and ^{13}C NMR spectra for m-dihydroxybenzene

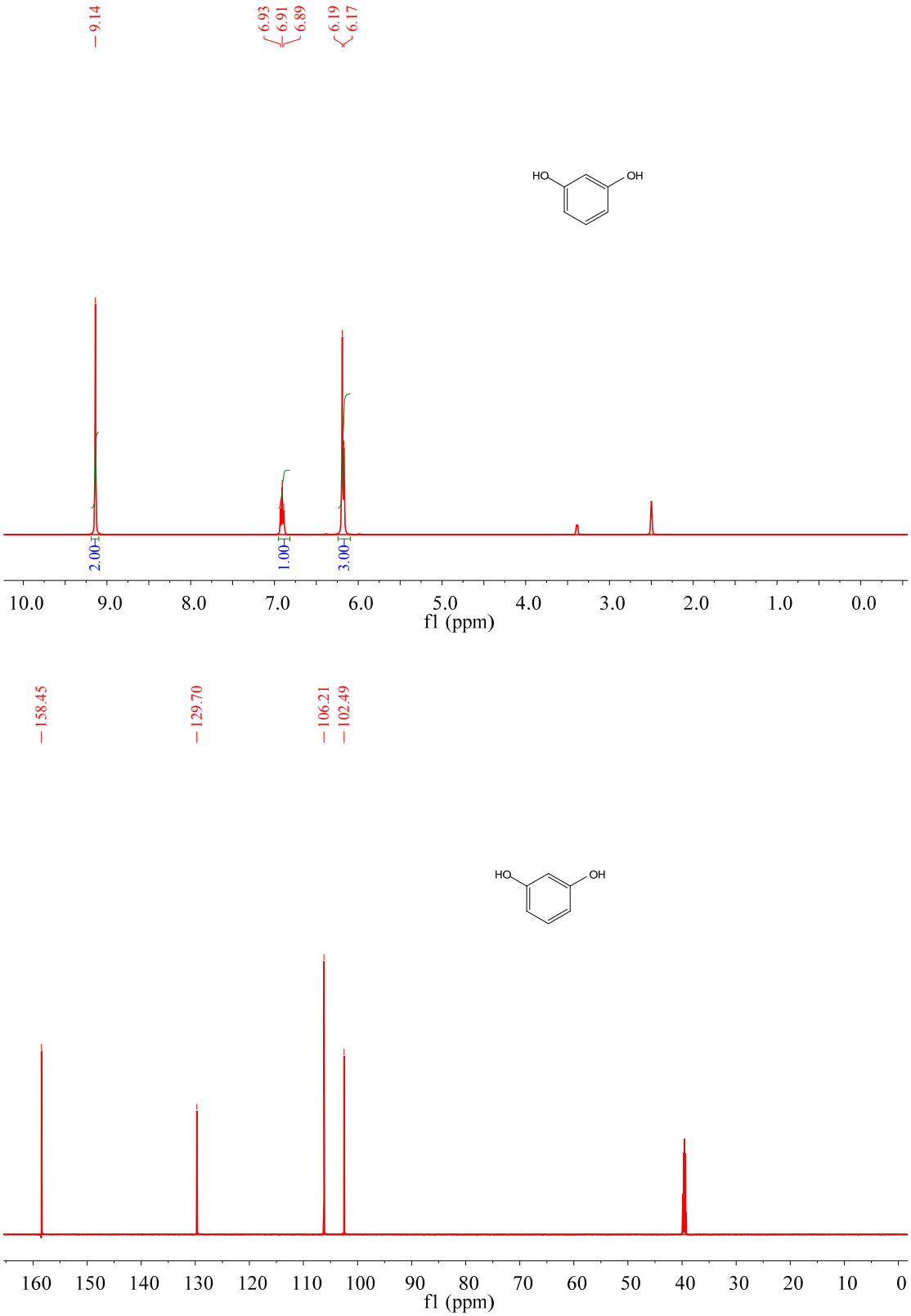

Fig. S37 The ^{1}H and ^{13}C NMR spectra for 4-ethylphenol